Taylor & Francis
Taylor & Francis Group

Experimental Mathematics

ISSN: 1058-6458 (Print) 1944-950X (Online) Journal homepage: http://www.tandfonline.com/loi/uexm20

Random Discrete Morse Theory and a New Library of Triangulations

Bruno Benedetti & Frank H. Lutz

To cite this article: Bruno Benedetti & Frank H. Lutz (2014) Random Discrete Morse Theory and a New Library of Triangulations, Experimental Mathematics, 23:1, 66-94, DOI: 10.1080/10586458.2013.865281

To link to this article: http://dx.doi.org/10.1080/10586458.2013.865281

Experimental Mathematics, 23(1):66–94, 2014

ISSN: 1058-6458 print / 1944-950X online
DOI: 10.1080/10586458.2013.865281

Random Discrete Morse Theory and a New Library of Triangulations

Bruno Benedetti[1] and Frank H. Lutz[2]
[1]Institut für Informatik, Freie Universität Berlin, Berlin, Germany
[2]Institut for Matematiske Fag, Københavns Universitet, København Ø, Denmark

CONTENTS

We introduce random discrete Morse theory as a computational scheme to measure the complexity of a triangulation. The idea is to try to quantify the frequency of discrete Morse matchings with few critical cells. Our measure will depend on the topology of the space, but also on how nicely the space is triangulated.

The scheme we propose looks for optimal discrete Morse functions with an elementary random heuristic. Despite its naiveté, this approach turns out to be very successful even in the case of huge inputs.

In our view, the existing libraries of examples in computational topology are "too easy" for testing algorithms based on discrete Morse theory. We propose a new library containing more complicated (and thus more meaningful) test examples.

1. INTRODUCTION

Libraries of objects for algorithm testing are extremely common in computational geometry. Their setup requires particular care: if a library consists of objects that are "too easy to understand," then basically any algorithm would score well on them, thus making it impossible for the researcher to appreciate the efficiency of the algorithms. Of course, agreeing on what examples should be regarded as easy is a hard challenge, and how to quantify complexity is even harder.

In the present paper, we focus on computational topology, which deals with simplicial complexes in an abstract manner, i.e., without prescribing a shape, a volume, or the dimension of a Euclidean space in which they embed. We present a possible random approach, which we call *random discrete Morse theory*. The mathematical background relies on Forman's discrete Morse theory from 1998 [Forman 98, Forman 02], which in turn builds on Whitehead's simple homotopy theory, developed around 1939 [Whitehead 39]. (Especially important is Whitehead's notion of collapsibility, which is a combinatorial strengthening of the contractibility property.)

2000 AMS Subject Classification: 57Q15, 57Q05, 57M25, 57N10, 57N13, 52B70, 52B05, 52B22, 55N35

Keywords: random discrete Morse theory, collapsibility, shellability, knots in triangulations, library of triangulations

Address correspondence to Frank H. Lutz, Institut for Matematiske Fag, Københavns Universitet, Universitetsparken 5, 2100 København Ø, Denmark. E-mail: lutz@math.ku.dk

Color versions of one or more of the figures in the article can be found online at www.tandfonline.com/uexm.

Our idea is to create a quantitative version of these two theories. For example, we would like to be able to tell not only whether a complex is collapsible, but also how "easy" it is to find a collapsing sequence. To give a mathematical basis to this intuition, we consider a random model whereby we perform elementary collapses completely at random. The probability of finding a complete collapsing sequence in this way will measure how easy it is to collapse the complex. Although this probability is, in most cases, too difficult to compute, we can estimate it empirically in polynomial time. The following elementary heuristic takes also into account complexes that are not contractible.

ALGORITHM: RANDOM DISCRETE MORSE

INPUT: A d-dimensional (abstract, finite) simplicial complex C, given by its list of facets.

(0) Initialize $c_0 = c_1 = \cdots = c_d = 0$.

(1) Is the complex empty? If yes, then STOP; otherwise, go to (2).

(2) Are there free codimension-one faces? If yes, go to (3); if no, go to (4).

(3) *Elementary Collapse*: Pick one free codimension-one face uniformly at random and delete it, together with the unique face that contains it. Go back to (1).

(4) *Critical Face*: Pick one of the top-dimensional faces uniformly at random and delete it from the complex. If i is the dimension of the face just deleted, increment c_i by 1 unit. Go back to (1).

OUTPUT: The resulting discrete Morse vector $(c_0, c_1, c_2, \ldots, c_d)$.

By construction, c_i counts the critical faces of dimension i. (We do not consider the empty face as a free face.) According to [Forman 98], every discrete Morse vector $(c_0, c_1, c_2, \ldots, c_d)$ is also the face vector of a cell complex homotopy equivalent to C.

Definition 1.1. The *discrete Morse spectrum* σ of a (finite) simplicial complex C is the collection of all possible resulting discrete Morse vectors produced by the algorithm RANDOM DISCRETE MORSE together with the distribution of the respective probabilities.

Example 1.2. Consider the graph A_7 of Figure 1. Since there are no free vertices in it, RANDOM DISCRETE MORSE picks an edge uniformly at random and deletes it. If the edge chosen is the central bridge (which happens with probability $\frac{1}{7}$), the output discrete Morse vector is $(2, 3)$. If any other edge than the central one is chosen, the output vector is $(1, 2)$. The discrete Morse spectrum is therefore $\{\frac{6}{7}\text{-}(1, 2), \frac{1}{7}\text{-}(2, 3)\}$; or $\{(1, 2), (2, 3)\}$ for short if we simply want to list the vectors of the spectrum.

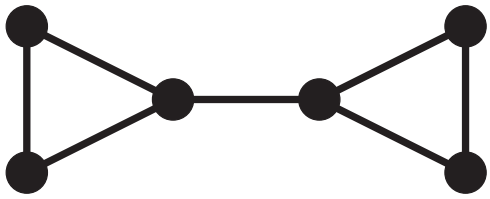

FIGURE 1. The graph A_7.

The algorithm RANDOM DISCRETE MORSE requires no backtracking, and it "digests" the complex very rapidly. The output $(1, 0, 0, \ldots, 0)$ is a certificate of collapsibility. If the output is different from $(1, 0, \ldots, 0)$, the complex could still be collapsible with a different sequence of free-face deletions.

RANDOM DISCRETE MORSE declares a k-face critical only if there are no free $(k-1)$-faces available. This keeps the number of faces declared critical to a minimum, thus making it more likely for the output vector to be optimal. Unfortunately, there are complexes on which the probability of achieving the optimal discrete Morse vector can be arbitrarily small; see Section 6 and also [Adiprasito et al. 14] for further discussion. But in case optimality is not reached, the algorithm still outputs something meaningful, namely (as already mentioned) the f-vector of a cell complex homotopy equivalent to the given complex.

Since the output arrives quickly, we can relaunch the program, say 10 000 times, possibly on separate computers (independently). The distribution of the obtained outcomes yields an approximation of the discrete Morse spectrum. By the so-called Morse inequalities, each output vector is componentwise greater than or equal to the vector of Betti numbers $(\beta_0, \ldots, \beta_d)$. When the spectrum stays "close" to the vector of Betti numbers, we can regard the triangulation as easy. This allows an empirical analysis of how complicated the complex is.

We point out that the problem of finding optimal discrete Morse functions (with as few critical cells as possible) is NP-hard [Joswig and Pfetsch 06, Lewiner et al. 03a]; even the decision problem whether some given (connected, finite) simplicial complex is collapsible is NP-complete [Tancer 12]. We therefore should not expect to find optimal discrete Morse vectors for any input immediately. Indeed, one can easily construct examples on which our (or similar) random heuristic performs poorly; see Section 6.

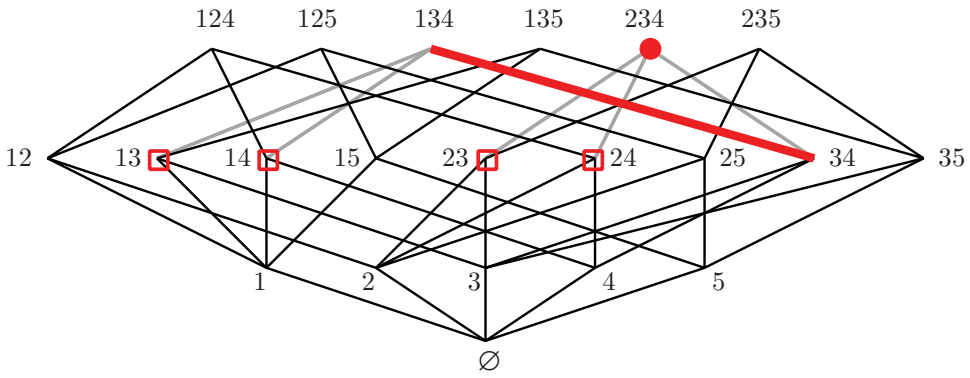

FIGURE 2. The Hasse diagram of the bipyramid with one critical triangle (234), one matching edge (34–134), and four free edges (13, 14, 23, 24) highlighted.

However, for many triangulations even of huge size, our elementary random heuristic produces optimal discrete Morse functions in almost 100% of the runs of the program. This could be interesting in the future also for homology computations. Discrete Morse functions (for general cell complexes) are implicitly computed in several homology algorithms that are based on fast (co)reduction techniques, such as the packages CHomP, RedHom, and Perseus.[1]

The paper is structured as follows: First we give details of our algorithm (Section 2) and compare it with previous approaches (Section 3). Then we survey the existing topological and combinatorial lower bounds for optimal discrete Morse vectors (Section 4). Finally, we describe and examine a collection of examples coming from several different areas of topology (Section 5). In our opinion, the resulting library (Section 7) is a richer and more sensitive testing ground for implementations based on discrete Morse theory.

2. DETAILS OF THE ALGORITHM AND COMPUTATIONAL COMPLEXITY

In the following, we give a more explicit description of our random heuristic. The first thing we do is to build the Hasse diagram of the given simplicial complex C, which represents the incidence structure of the face poset of C; see Figure 2 for an example. It takes $O(d \cdot I \cdot T)$ steps to construct the Hasse diagram of a simplicial complex if the complex is given by its facets (or to be precise, by its vertex–facet incidences). Here d is the dimension of the input complex, T the total number of faces, and I the number of vertex–facet incidences [Kaibel and Pfetsch 02]; cf. also [Kaibel and Pfetsch 03].

[1]Available respectively at chomp.rutgers.edu, redhom.ii.uj.edu.pl, math.rutgers.edu/~vidit/perseus.html.

Once the upward Hasse diagram and the downward Hasse diagram are set up (see below), we deconstruct a copy of the upward Hasse diagram in every run of our program by deleting (randomly chosen) critical faces or pairs of faces in case there are free faces. We illustrate this with a concrete example.

Example 2.1. (The bipyramid.) The 2-dimensional boundary of the bipyramid of Figure 3 has six triangles, nine edges, and five vertices. We list the faces levelwise in lexicographic order and identify each face by a label k^i denoting the kth face of dimension i in the respective lexicographic list:

1^2: [1,2,4], 2^2: [1,2,5], 3^2: [1,3,4], 4^2: [1,3,5], 5^2: [2,3,4], 6^2: [2,3,5],

1^1: [1,2], 2^1: [1,3], 3^1: [1,4], 4^1: [1,5], 5^1: [2,3], 6^1: [2,4], 7^1: [2,5], 8^1: [3,4], 9^1: [3,5],

1^0: [1], 2^0: [2], 3^0: [3], 4^0: [4], 5^0: [5].

Next, we initialize the Hasse diagram, whereby the graph of the Hasse diagram is stored twice. In the *upward Hasse*

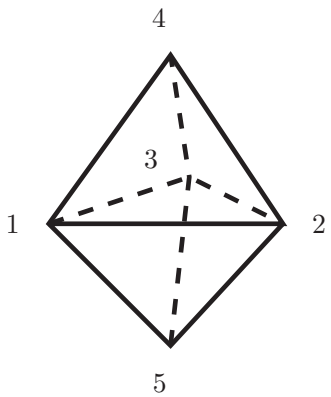

FIGURE 3. The bipyramid.

diagram, we list levelwise all inclusions of i-dimensional faces in $(i+1)$-dimensional faces,

$i = 1$: $1^1 \nearrow \{1^2, 2^2\}$, $2^1 \nearrow \{3^2, 4^2\}$, $3^1 \nearrow \{1^2, 3^2\}$,
$4^1 \nearrow \{2^2, 4^2\}$, $5^1 \nearrow \{5^2, 6^2\}$, $6^1 \nearrow \{1^2, 5^2\}$,
$7^1 \nearrow \{2^2, 6^2\}$, $8^1 \nearrow \{3^2, 5^2\}$, $9^1 \nearrow \{4^2, 6^2\}$,

$i = 0$: $1^0 \nearrow \{1^1, 2^1, 3^1, 4^1\}$, $2^0 \nearrow \{1^1, 5^1, 6^1, 7^1\}$,
$3^0 \nearrow \{2^1, 5^1, 8^1, 9^1\}$, $4^0 \nearrow \{3^1, 6^1, 8^1\}$,
$5^0 \nearrow \{4^1, 7^1, 9^1\}$,

while in the *downward Hasse diagram* we list levelwise the $(j-1)$-dimensional faces that are contained in the j-dimensional faces,

$j = 2$: $1^2 \searrow \{1^1, 3^1, 6^1\}$, $2^2 \searrow \{1^1, 4^1, 7^1\}$,
$3^2 \searrow \{2^1, 3^1, 8^1\}$, $4^2 \searrow \{2^1, 4^1, 9^1\}$,
$5^2 \searrow \{5^1, 6^1, 8^1\}$, $6^2 \searrow \{5^1, 7^1, 9^1\}$,

$j = 1$: $1^1 \searrow \{1^0, 2^0\}$, $2^1 \searrow \{1^0, 3^0\}$, $3^1 \searrow \{1^0, 4^0\}$,
$4^1 \searrow \{1^0, 5^0\}$, $5^1 \searrow \{2^0, 3^0\}$, $6^1 \searrow \{2^0, 4^0\}$,
$7^1 \searrow \{2^0, 5^0\}$, $8^1 \searrow \{3^0, 4^0\}$, $9^1 \searrow \{3^0, 5^0\}$.

Here, $3^1 \nearrow \{1^2, 3^2\}$ is shorthand notation for the inclusion of the edge 3^1: [1,4] in the two triangles 1^2: [1,2,4] and 3^2: [1,3,4].

During each run, the downward Hasse diagram is maintained, while a copy of the upward Hasse diagram is updated after the removal of a critical face or a pair consisting of a free face and the unique face in which it is contained. The sequence of updating steps for the above example could be as follows:

0. `compute downward and upward Hasse diagram`
1. `initialize copy of the upward Hasse diagram`
2. `free edges`: none
3. `select random critical triangle`: 5^2: [2,3,4]
4. `update upward Hasse diagram`:

$i = 1$: $1^1 \nearrow \{1^2, 2^2\}$, $2^1 \nearrow \{3^2, 4^2\}$, $3^1 \nearrow \{1^2, 3^2\}$,
$4^1 \nearrow \{2^2, 4^2\}$, $5^1 \nearrow \{6^2\}$, $6^1 \nearrow \{1^2\}$,
$7^1 \nearrow \{2^2, 6^2\}$, $8^1 \nearrow \{3^2\}$, $9^1 \nearrow \{4^2, 6^2\}$

5. `free edges`: $5^1, 6^1, 8^1$
6. `select random free edge`: 8^1: [3,4] `paired with` 3^2: [1,3,4]
7. `update upward Hasse diagram`:

$i = 1$: $1^1 \nearrow \{1^2, 2^2\}$, $2^1 \nearrow \{4^2\}$, $3^1 \nearrow \{1^2\}$,
$4^1 \nearrow \{2^2, 4^2\}$, $5^1 \nearrow \{6^2\}$, $6^1 \nearrow \{1^2\}$,
$7^1 \nearrow \{2^2, 6^2\}$, $8^1 \nearrow \{\}$, $9^1 \nearrow \{4^2, 6^2\}$,

$i = 0$: $1^0 \nearrow \{1^1, 2^1, 3^1, 4^1\}$, $2^0 \nearrow \{1^1, 5^1, 6^1, 7^1\}$,
$3^0 \nearrow \{2^1, 5^1, 9^1\}$, $4^0 \nearrow \{3^1, 6^1\}$,
$5^0 \nearrow \{4^1, 7^1, 9^1\}$

8. `free edges`: $2^1, 3^1, 5^1, 6^1$
9. ...

The downward Hasse diagram tells us precisely which parts of the upward Hasse diagram we have to update. For example, the choice of the critical triangle 5^2: [2,3,4] forces us to update, via $5^2 \searrow \{5^1, 6^1, 8^1\}$, the inclusions of the edges $5^1, 6^1, 8^1$ in the upward Hasse diagram (by removing the triangle 5^2 as including face).

Triangulations of closed manifolds initially have no free faces. Thus, we start with an empty list of free faces and immediately remove a random critical face. For triangulations of manifolds with boundary or general simplicial complexes, we first have to initialize the list of free faces. (This extra computation time can be seen by comparing the respective run times for the examples `knot` and `nc_sphere` in Table 6 (see also Section 5.5): At 0.813 seconds, the 3-ball `knot` takes slightly longer per round than the 3-sphere `nc_sphere` at 0.470 seconds.)

Whenever we are done with one level of the Hasse diagram, we initialize the set of free faces for the next level below. Besides updating the upward Hasse diagram in each round, we also keep track of the following:

1. The current *list of free faces* (and we update this list whenever we delete a critical face or a pair consisting of a free face and the unique face in which it is contained).
2. The current *discrete Morse vector* $(c_0, c_1, \ldots, c_d)$ (which is initialized by $(0, 0, \ldots, 0)$ and updated by incrementing c_i by one whenever a critical face of dimension i is selected).

At the end of every round, the resulting discrete Morse vector $(c_0, c_1, \ldots, c_d)$ is stored along with its number of appearances in the various rounds. Eventually, we output the list of all obtained discrete Morse vectors together with their frequencies.

2.1. Implementation in GAP

We implemented our random heuristic in GAP. In particular, we used GAP operations on lists and sets to initialize and update Hasse diagrams and respective lists of free faces. Our implementation is basic and has roughly 150 lines of code.

The largest complex (in terms of number of faces) on which we tested our program has face vector $f = (5013, 72300, 290944, 495912, 383136, 110880)$. For this triangulation [Adiprasito et al. 14] of a contractible 5-manifold different from a 5-ball, it took in total 60 : 17 : 33 + 21 : 41 : 31 h : min : sec first to build the Hasse diagram and then to run the random heuristic once. As resulting discrete Morse vector we obtained $(1, 0, 0, 0, 0, 0)$; thus, this nontrivial 5-manifold is collapsible [Adiprasito et al. 14].

We point out that there is considerable room for improvement with respect to computation time. First of all, the Hasse diagram of a complex can be stored in terms of (sparse)

boundary matrices on which fast elimination steps represent elementary collapses; see [Joswig 04] for a discussion. In addition, it is much faster to perform matrix operations in, say, C++ than to carry out elementary set operations in GAP. However, for computing (respectively simplifying a presentation of) the fundamental group of a simplicial complex, GAP provides efficient heuristics; cf. Section 5.10.

3. COMPARISON WITH OTHER ALGORITHMS

There are three main previous algorithmic approaches that aim to compute optimal discrete Morse functions for simplicial complexes: one from [Joswig and Pfetsch 06], one from [Engström 09], and one from [Lewiner et al. 03a] (cf. also [Lewiner 05]).

Tools that make it possible to improve discrete Morse functions were provided by [Hersh 05], while how to improve discrete Morse functions for geometric complexes in $\mathbb{R}^3$ was discussed in [King et al. 05].

A completely different random approach to discrete Morse theory was attempted in [Nicolaescu 12]. Essentially, Nicolaescu tried to choose edges in the Hasse diagram randomly to obtain discrete Morse matchings, but he showed that this approach will not be successful. Indeed, choosing edges in the Hasse diagram at random will produce bottlenecks even for complexes that are easily collapsible.

3.1. The Algorithm of Joswig and Pfetsch

This deterministic algorithm, apart from a complete backtrack search, is currently the only available implementation that actually determines optimal discrete Morse functions for all inputs. In the approach of [Joswig and Pfetsch 06], the problem of finding an optimal discrete Morse function is translated into a maximal matching problem for the underlying graph of the Hasse diagram with an additional acyclicity condition [Chari 00, Forman 98]. The acyclic matching problem is then solved as an integer linear program.

For various small instances, the Joswig–Pfetsch approach successfully produces optimal discrete Morse functions. The first case, however, in which the associated integer linear program was too large to handle is the 16-vertex triangulation `poincare` [Björner and Lutz 00] of the Poincaré homology 3-sphere with $f = (16, 106, 180, 90)$. Joswig and Pfetsch interrupted the computation after one week (although because they did not make use of the fact that at least six critical cells are necessary, since the fundamental group of the Poincaré homology 3-sphere is acyclic; cf. Section 5.9). For the same instance, our heuristic found the optimal Morse vector $(1, 2, 2, 1)$ within 0.02 seconds. Also, for other small instances our heuristic was much faster. For example, for Rudin's ball `rudin` [Rudin 58, Wotzlaw 05] with $f = (14, 66, 94, 41)$, Joswig and Pfetsch needed 103.78 seconds to achieve the optimal discrete Morse vector $(1, 0, 0, 0)$, while our heuristic found the optimum in 0.004+0.00107 seconds; cf. Section 5.5.

3.2. Engström's Approach

The heuristic approach of [Engström 09] is elegant and fast. Roughly speaking, the idea is to proceed by deleting vertex stars rather than by deleting pairs of faces. Engström introduces what he calls "Fourier–Morse theory," a theory based on Kahn–Saks–Sturtevant's notion of nonevasiveness, much like Forman's discrete Morse theory was based on Whitehead's notion of collapsibility. Instead of computing discrete Morse functions, Engström's heuristic computes Fourier–Morse functions, which are certain discrete Morse functions, but not necessarily the optimal ones among them. In particular, obtaining an output $(1, 0, \ldots, 0)$ with this approach yields a certificate of nonevasiveness, a stronger property than collapsibility; cf. [Kahn et al. 84].

However, there is a 3-ball with only 12 vertices that has the collapsibility property, but not the nonevasiveness property [Benedetti and Lutz 13a]. As for other examples, Engström obtains $(1, 5, 5, 1)$ as a discrete Fourier–Morse vector for the 16-vertex triangulation of the Poincaré homology 3-sphere `poincare`. However, the optimal discrete Morse vector for this example is $(1, 2, 2, 1)$. For Rudin's ball `rudin`, Engström found $(1, 2, 2, 0)$, compared to the optimum $(1, 0, 0, 0)$. Engström's implementation depends on the vertex-labeling of a complex. For a fixed labeling, the optimal discrete Morse vector is often missed, even on triangulations of relatively small size.

3.3. The Heuristic of Lewiner, Lopes, and Tavares

The heuristic approach of [Lewiner et al. 03a] (cf. also [Lewiner 05]) is fast. It was used to produce optimal discrete Morse vectors for several large 2- and 3-dimensional complexes. The problem of finding optimal discrete Morse vectors is reformulated in terms of finding maximal hyperforests of hypergraphs. Then different greedy heuristics are used to obtain large hyperforests.

It must be remarked, though, that most of the instances listed in [Lewiner et al. 03a] and later in [Lewiner 05] are mostly harmless from the point of view of discrete Morse theory; they are mainly 2-dimensional surfaces or shellable 3-dimensional balls and spheres, or products thereof, with the exception of the three more complicated examples `knot`, `nc_sphere`, and `bing` from Hachimori's simplicial complex library [Hachimori 01].

It is precisely on these three examples that the greedy heuristics of Lewiner et al. produce somewhat inconsistent results.

In [Lewiner et al. 03a], (1, 1, 1, 0) was obtained for `bing` and `knot`. In [Lewiner 05, p. 92], `bing` and `knot` appear with (1, 0, 0, 0) with no mention of the improvement with respect to [Lewiner et al. 03a]. Moreover, `nc_sphere` is listed in [Lewiner 05, p. 92] with (1, 2, 2, 1), and on p. 89 is noted, "Trickier, the nonshellable 3-sphere (NC Sphere) is a delicate model since no discrete Morse function can reach the minimal number of critical points for smooth homotopy." This latter statement is false, for we found (in 12 out of 10 000 runs) the optimal discrete Morse vector (1, 0, 0, 1) for `nc_sphere`; cf. Table 8. In fact, the 3-sphere `nc_sphere` with $f = (381, 2309, 3856, 1928)$ is obtained from the 3-ball `knot` with $f = (380, 1929, 2722, 1172)$ by adding a cone over the boundary of `knot`. By this, every discrete Morse function on `knot` with discrete Morse vector (1, 0, 0, 0) can be used to produce a discrete Morse function with discrete Morse vector (1, 0, 0, 1) on `nc_sphere`. In contrast, it would theoretically be possible to have `knot` with optimal discrete Morse vector (1, 1, 1, 0), while `nc_sphere` has optimal discrete Morse vector (1, 0, 0, 1). The best discrete Morse vector we found in 1 000 000 runs for `knot` is (1, 1, 1, 0), see Table 6, whereas as mentioned above, [Lewiner 05] seemed to claim (1, 0, 0, 0) for this example, which would beat our algorithm.

4. THEORETICAL LOWER BOUNDS FOR DISCRETE MORSE VECTORS

In this section, we briefly recall some theoretical lower bounds for minimal discrete Morse vectors. The obstructions for the existence of discrete Morse functions with a certain number of critical cells are of various natures. Here we basically use four different criteria. The first concerns ridge–facet incidences, the second follows from elementary algebraic topology (applied to the Morse complex), the third uses knot theory, and the fourth comes from smooth Morse theory.

4.1. Ridge–Facet Incidences and Euler Characteristic

In order for a collapse to begin, there need to be free faces. This is how to create a first obstruction, namely by constructing d-dimensional triangulations in which every $(d-1)$-face is contained in two or more d-faces.

The most famous example of this type is the dunce hat, a contractible 2-complex obtained from a single triangle by identifying all three boundary edges in a noncoherent way. In any triangulation of the dunce hat, each edge belongs to either two or three triangles; cf. [Benedetti and Lutz 13b]. Hence, the dunce hat cannot be collapsible, or in other words, it cannot have (1, 0, 0) as discrete Morse vector.

The vectors (1, 0, 1) and (1, 1, 0) are also forbidden for the dunce hat. In fact, since each elementary collapse deletes two faces of consecutive dimensions, it does not change the Euler characteristic. In particular, the alternating sum of the entries of a discrete Morse vector should always be equal to the Euler characteristic of a complex.

The dunce hat does, however, admit (1, 1, 1) as discrete Morse vector, which is therefore optimal.

4.2. The Morse Complex

Forman showed that every discrete Morse vector on a simplicial complex C is also the face vector of a *model* for C, that is, a CW complex homotopy equivalent to C.

Theorem 4.1. [Forman 02] *Assume that some d-complex C admits a discrete Morse function with c_i critical faces of dimension i, $i = 0, \dots, d$. Then C has a model with c_i i-cells, called a* Morse complex.

This theorem results in several obstructions. First of all, the ith (rational) Betti number of an arbitrary CW complex is always bounded above by its number of i-dimensional cells.

Corollary 4.2. (Forman's weak Morse inequalities.) [Forman 02] *Assume that some d-complex C admits a discrete Morse function with c_i critical faces of dimension i, $i = 0, \dots, d$. Then $c_i \geq \beta_i(C)$ for each i.*

The previous result still holds if we consider homology over a finite field.

Corollary 4.3. *Assume that some d-complex C admits a discrete Morse function with c_i critical faces of dimension i, $i = 0, \dots, d$. Then $c_i \geq \dim H_i(C; \mathbb{Z}_p)$ for each i and for each prime p.*

Sometimes, it is convenient to focus on homotopy groups rather than on homology groups. Recall that the fundamental group of a CW complex with one 0-cell is completely determined by its 2-skeleton; a presentation of the group can be obtained using the 1-cells as generators and the 2-cells as relators. In particular, if the CW complex has no 1-cells, its fundamental group must be trivial; and if the CW complex has only one 1-cell, its fundamental group must be trivial or cyclic.

Corollary 4.4. *Assume that some d-complex C with fundamental group G admits a discrete Morse function with one*

critical face of dimension 0 *and* c_1 *critical faces of dimension* 1. *Then* $c_1 \geq \operatorname{rank}(G)$*, the minimal number of generators in a presentation of* G. *(In particular, if* G *is nonabelian, then* $c_1 \geq 2$*.)*

4.3. Knot-Theoretic Obstructions

Obstructions arising from short knots were considered first in [Bing 64], [Goodrick 68], and [Lickorish 91], and later investigated in [Benedetti 12, Benedetti and Lutz 13a, Lutz 04b], among others. Recall that a knot K inside a triangulation of a 3-sphere is just a 1-dimensional subcomplex homeomorphic to a 1-sphere (or in other words, a closed path in the 1-skeleton). The *knot group* is the fundamental group of the knot complement inside the sphere. Knot groups are perhaps the main invariant in knot theory.

In the simplest form (that is, for 3-dimensional spheres), the obstructions are of the following type:

Theorem 4.5. [Lickorish 91]; cf. also [Benedetti 12] *Assume that some triangulated* 3*-sphere* S *admits some discrete Morse function with* c_2 *critical* 2*-faces. Then for every knot* K *inside* S*, one has*

$$c_2 \geq \operatorname{rank}(G_K) - f_1(K),$$

where G_K *is the knot group of* K *and* $f_1(K)$ *is the number of edges of* K.

Theorem 4.5 is usually applied together with the following two well-known facts:

(1) There are knots whose groups have arbitrarily high rank; for example, the knot group of a connected sum of m trefoils has rank $\geq m + 1$ [Goodrick 68].

(2) Every knot can be realized with only three edges in a suitably triangulated 3-sphere [Bing 64].

In particular, if we consider a 3-sphere S containing the connected sum of three trefoils realized on three edges, then Theorem 4.5 yields $c_2 \geq 1$ for all discrete Morse vectors $(1, c_1, c_2, 1)$. Note that $c_1 = c_2$, for Euler characteristic reasons.

A similar statement can be proven for 3-dimensional balls.

Theorem 4.6. [Benedetti 12, Corollary 4.25] *Assume that some triangulated* 3*-ball* B *admits some discrete Morse function with* c_1 *critical edges. Let* K *be a knot in the* 1*-skeleton of* B*, realized as a path of* b *edges in the boundary of* B *plus a path of* $e = f_1(K) - b$ *interior edges. Then*

$$c_1 \geq \operatorname{rank}(G_K) - 2e,$$

where G_K *is the knot group of* K.

4.4. Morse-Theoretic Obstructions

Very recently, the first author proved the following result for smooth manifolds.

Theorem 4.7. [Benedetti 13] *Every smooth Morse vector is also a discrete Morse vector on some (compatible) PL triangulation. In dimensions up to* 7*, the converse holds as well.*

The converse statement is interesting for us because it yields further obstructions. For example, we know from [Boileau and Zieschang 84] and others that for every $r > 0$, there is a (smooth) 3-manifold M_r of Heegaard genus $g \geq \operatorname{rank}(M_r) + r$. It follows that for every PL triangulation T of M_r, every discrete Morse vector on T has $c_1 \geq g \geq \operatorname{rank}(M_n) + r$ critical edges.

5. TOWARD A NEW LIBRARY OF TRIANGULATIONS

Tables 3–10 provide a library of 45 instances for which we sampled the discrete Morse spectrum. We ran our random algorithm 10 000 rounds on each example, except for eight examples for which we did fewer runs. The 45 examples were selected for different reasons, as we will explain below. The respective examples are listed at the beginning of each subsection.[2]

An additional infinite series of complicated triangulations, based on a handlebody construction of [Akbulut and Kirby 85], was recently given in [Tsuruga and Lutz 13].

5.1. "Trivial" Triangulations

`Examples: dunce_hat, d2n12g6, regular_2_21_23_1`

Discrete Morse theory is trivial on 1-dimensional complexes (graphs) and 2-dimensional compact manifolds (surfaces); cf. [Lewiner et al. 03a]. A simple modification of our heuristic allows us to incorporate this as follows. Once we have reduced a simplicial complex to a 1-dimensional complex, we switch to a deterministic strategy: as long as there are edges that are contained in a cycle, delete such (critical) edges iteratively; then collapse the remaining tree (or forest) to a point (respectively collection of points).

Definition 5.1. Let C be a connected finite simplicial complex. The *normalized discrete Morse spectrum* σ_N of C is obtained from the discrete Morse spectrum σ of C by normalizing every discrete Morse vector $(c_0, c_1, c_2, \ldots, c_d)$ in the spectrum to

[2]The library of examples can be found online at http://page.math.tu-berlin.de/~lutz/stellar/library_of_triangulations/.

$(1, c_1 - c_0 + 1, c_2, \ldots, c_d)$ and summing the probabilities for the original vectors that have the same normalization.

Example 5.2. The graph A_7 of Figure 1 has normalized discrete Morse spectrum {1-(1, 2)} or, for short, {(1, 2)}.

We introduce the following averages:

1. c_σ, the average number of critical cells for the vectors in the discrete Morse spectrum σ of a simplicial complex C.
2. c_σ^N, the average number of critical cells for the vectors in the normalized discrete Morse spectrum σ_N of C.

By Corollary 4.2, we have

$$c_\sigma \;\geq\; c_\sigma^N \;\geq\; \beta_0 + \beta_1 + \cdots + \beta_d.$$

The coefficient c_σ^N (and also c_σ) is of some interest if we want to reduce the size of a complex randomly as a preprocessing step for homology computations; it gives an estimate for the number of cells that we are left with for the Smith normal form computations.

Lemma 5.3. *Every connected simplicial* 1*-complex K with n vertices and $m \geq n - 1$ edges has normalized discrete Morse spectrum* $\{(1, m - n + 1)\}$ *and* $c_\sigma^N = 2 + m - n$.

The homology vector in this case is $H_*(K) = (\mathbb{Z}, \mathbb{Z}^{m-n+1})$, so the weak discrete Morse inequalities (see Corollary 4.2) are sharp.

Lemma 5.4. *Every triangulation K of a closed (connected) surface of Euler characteristic χ has normalized discrete Morse spectrum* $\{(1, 2 - \chi, 1)\}$*, and* $c_\sigma^N = 4 - \chi$*. More generally, the same holds for every strongly connected* 2*-complex K without free edges.*

Proof. Triangulations of surfaces are strongly connected. Hence after the removal of only one critical triangle, the remaining complex collapses onto a 1-dimensional complex, i.e., $c_2 = 1$. The conclusion follows from the previous lemma and extends to all strongly connected 2-complexes K without free edges. □

The example `d2n12g6` in Table 3 is the unique vertex-transitive, vertex-minimal neighborly triangulation of the orientable surface of genus 6 [Altshuler et al. 96]. The example `regular_2_21_23_1` is a regular triangulation of the orientable surface of genus 15 with 21 vertices [Lutz 99, Chapter 5].

Something can also be said about complexes with few vertices:

Theorem 5.5. [Bagchi and Datta 05] *Every $\mathbb{Z}_2$-acyclic simplicial complex with at most seven vertices is collapsible.*

Corollary 5.6. *Every $\mathbb{Z}_2$-acyclic simplicial complex K with at most seven vertices is extendibly collapsible and therefore has trivial discrete Morse spectrum* $\{(1, 0, 0)\}$ *with* $c_\sigma = c_\sigma^N = 1$.

The seven-vertex bound is sharp; the triangulation `dunce_hat` (cf. [Benedetti and Lutz 13b]) of the dunce hat is an eight-vertex example of a noncollapsible contractible complex.

5.2. 3-Manifolds with up to 10 Vertices

For all 250 359 examples in the catalog [Lutz 08] of triangulations of 3-manifolds with up to 10 vertices, optimal discrete Morse vectors were found by a single run of our program each; see Table 1.

Theorem 5.7. *All* 250 359 *examples of triangulated* 3*-manifolds with up to* 10 *vertices admit a perfect discrete Morse function.*

The spheres in this list are all shellable, as are all 3-spheres with up to 11 vertices [Sulanke and Lutz 09]. The smallest known nonshellable 3-sphere, `S_3_13_56` (`trefoil`), has 13 vertices [Lutz 04b]. For all the 1134 nonspherical examples, the statement of the theorem is new.

Vertices\Types	S^3	$S^2 \times S^1$	$S^2 \times S^1$	All	Total Time (in Min:Sec.Frac)
5	1	–	–	1	0.008
6	2	–	–	2	0.008
7	5	–	–	5	0.012
8	39	–	–	39	0.060
9	1 296	1	–	1 297	3.836
10	247 882	615	518	249 015	17:35.606

TABLE 1. Total time to find optimal discrete Morse functions (in a single run) for each of the combinatorial 3-manifolds with up to 10 vertices.

5.3. Polytopal Spheres

Examples: S_3_100_4850, 600_cell, S_3_1000_2990, S_5_100_472.

We ran our program on the 3-dimensional boundary S_3_100_4850 of the cyclic 4-polytope with 100 vertices and 4850 facets, on the 3-dimensional boundary 600_cell of the 600-cell, on the 3-dimensional boundary S_3_1000_2990 of a stacked 4-polytope with 1000 vertices and 2990 facets, and on the 4-dimensional boundary S_5_100_472 of a stacked 5-polytope with 100 vertices and 472 facets. In all these cases, we obtained the optimal discrete Morse vector $(1, 0, \ldots, 0, 1)$ in 10 000 out of 10 000 attempts. We also tested various other examples of simplicial polytopal spheres, and we always observed a trivial spectrum in these experiments. However, the normalized discrete Morse spectrum of simplicial polytopal spheres is not trivial in general.

Theorem 5.8. [Crowley et al. 03] *The 7-simplex Δ_7 with eight vertices contains in its 2-skeleton an eight-vertex triangulation of the dunce hat onto which it collapses.*

As a direct consequence of Theorem 5.8, the 7-simplex Δ_7 is not extendibly collapsible. Therefore, the spectrum of its boundary is nontrivial. Similarly, the simplicial polytopal Grünbaum–Sreedharan 3-sphere No. 32 on eight vertices, which contains a dunce hat [Benedetti and Lutz 13b], has nontrivial Morse spectrum; see the example dunce_hat_in_3_ball in Section 5.5 below.

5.4. Random Spheres

Example: S_3_50_1033.

While random surfaces can easily be generated, we lack good random models for 3- or higher-dimensional manifolds; cf. [Dunfield and Thurston 06]. One possible approach is to consider all triangulations of 3-spheres or 3-manifolds with a fixed number n of vertices, with the uniform distribution. While this setting is very promising for performing random experiments, we need to get a hold on the set of all the triangulations with n vertices in the first place, a task that so far has been solved only for 3-manifolds with up to 11 vertices [Sulanke and Lutz 09].

Another model can be derived by performing random walks on the set of all triangulations whereby each step is represented by a single bistellar flip. According to a theorem of [Pachner 87], two distinct triangulations of a manifold are PL homeomorphic if and only if they can be connected by a sequence of bistellar flips. An implementation of bistellar flips for exploring the space of triangulations within one PL component is the program BISTELLAR; see [Björner and Lutz 00] for a program description.[3] The bistellar flip approach for generating random triangulations depends on the number of executed flips as well as on the way the flips are chosen. As a consequence, triangulations with n vertices are not selected according to the uniform distribution.

For the example S_3_50_1033, we started with the boundary of the cyclic 4-polytope with 50 vertices and face vector $f = (50, 1225, 2350, 1175)$. We then applied 1500 bistellar 1-flips and reverse 1-flips that were chosen randomly from all admissible flips. The resulting sphere S_3_50_1033 has f-vector (50, 1083, 2066, 1033). The average number of critical cells in 10 000 runs turned out experimentally to be roughly 3.2 (which is considerably larger than 2). We therefore can conclude heuristically that random spheres tend to have a nontrivial spectrum.

5.5. Knotted Triangulations of Balls and Spheres

Examples: dunce_hat_in_3_ball, Barnette_sphere, B_3_9_18, trefoil_arc, trefoil, rudin, double_trefoil_arc, double_trefoil, triple_trefoil_arc, triple_trefoil, non_4_2_colorable, knot, nc_sphere, bing.

The example dunce_hat_in_3_ball [Benedetti and Lutz 13b] is a triangulated 3-ball that contains the eight-vertex triangulation dunce_hat in its 2-skeleton. To get stuck with dunce_hat, we need to perform collapses without removing any of the 17 triangles of the dunce hat. This results in a low probability of getting stuck. Indeed, in 1 000 000 runs, we always found $(1, 0, 0, 0)$ as resulting discrete Morse vector.

The nonpolytopal Barnette_sphere [Barnette 73] with eight vertices also has trivial observed spectrum: In 1 000 000 runs of our program, we obtained the optimal discrete Morse vector $(1, 0, 0, 1)$. For the nonshellable 3-ball B_3_9_18 [Lutz 04a] with 9 vertices and Rudin's nonshellable 3-ball rudin [Rudin 58, Wotzlaw 05] with 14 vertices, we achieved the optimal discrete Morse vector $(1, 0, 0, 0)$ in every run. Therefore, nonpolytopality and nonshellability do not necessarily cause a nontrivial observed spectrum.

If we wish to construct triangulated balls or spheres of small size with a very nontrivial observed spectrum, we need to build in complicated substructures of small size (like complicated knots on few edges) at which to get stuck.

The triangulated 3-sphere trefoil (S_3_13_56 [Lutz 04b]) contains a 3-edge trefoil knot in its 1-skeleton and has optimal discrete Morse vector $(1, 0, 0, 1)$. This vector was obtained in roughly 96% of the runs of our heuristic.

[3] BISTELLAR is available at http://page.math.tu-berlin.de/~lutz/stellar/BISTELLAR.

trefoil	2.0778	double_trefoil	3.5338	triple_trefoil	5.9898
trefoil_bsd	2.0202	double_trefoil_bsd	3.3414	triple_trefoil_bsd	5.7352

TABLE 2. Average number of critical cells for the knotted spheres and their barycentric subdivisions, based on 10 000 random runs.

The triangulated 3-sphere double_trefoil (S_3_16_92 [Benedetti and Lutz 13a]) with optimal discrete Morse vector (1, 0, 0, 1) has a three-edge double trefoil knot in its 1-skeleton. Here, (1, 0, 0, 1) was achieved in only 40% of the runs. The triangulated 3-sphere triple_trefoil (S_3_18_125 [Benedetti and Lutz 13a]) contains a three-edge triple trefoil knot in its 1-skeleton and has optimal discrete Morse vector (1, 1, 1, 1), which we found 31% of the time.

The 3-ball trefoil_arc is obtained from the 3-sphere trefoil by deleting the star of a vertex. It contains the trefoil knot as a spanning arc and has optimal discrete Morse vector (1, 0, 0, 0). The deletion of the star of a vertex from the 3-sphere double_trefoil yields the 3-ball double_trefoil_arc with the double trefoil knot as spanning arc and optimal discrete Morse vector (1, 1, 1, 0).

For the triple trefoil knot, the deletion of a vertex from the 3-sphere triple_trefoil yields the 3-ball triple_trefoil_arc, for which the optimal discrete Morse vector is (1, 2, 2, 0); see Theorem 4.6. We found this vector in about 60% of the runs.

A larger 3-ball, knot, that has the trefoil knot as spanning arc was constructed (via a pile of cubes) in [Hachimori 01]. The best discrete Morse vector we found for knot is (1, 1, 1, 0). It might well be that knot admits (1, 0, 0, 0) as optimal discrete Morse vector. The nonconstructible 3-sphere nc_sphere [Hachimori 01] is obtained from knot by adding the cone over the boundary of knot. For this example, we found (1, 0, 0, 1) as optimal discrete Morse vector, but in only 12 out of 10 000 runs.

The triangulation bing is a 3-dimensional thickening of Bing's house with two rooms [Bing 64] due to [Hachimori 01] (again, via a pile of cubes). It is a 3-ball with 480 vertices for which we found (1, 0, 0, 0) as optimal discrete Morse vector in only seven out of 10 000 runs. We therefore can regard this ball as *barely collapsible*.

A non-(4, 2)-colorable triangulation of the 3-sphere, non_4_2_colorable, was constructed in [Lutz and Møller 14] with 167 vertices using 10 copies of the double trefoil knot. The best discrete Morse vector we found once for this example in 10 000 runs is (1, 2, 2, 1), whereas with the rev_lex heuristic of Section 7 we found (1, 0, 0, 1) for this example; see Table 11. The average number of critical cells for non_4_2_colorable computed and normalized over only 10 random runs (for the sake of simplicity) as listed in Table 5 is roughly 25.2.

5.6. Barycentric Subdivisions

Examples: trefoil_bsd, double_trefoil_bsd, triple_trefoil_bsd.

Interestingly, the barycentric subdivisions trefoil_bsd, double_trefoil_bsd, and triple_trefoil_bsd of the knotted spheres trefoil, double_trefoil, and triple_trefoil, respectively, have a lower observed spectrum than the corresponding original spheres; compare Table 2.

5.7. Standard and Exotic PL Structures on 4-Manifolds

Examples: CP2, RP4, K3_16, K3_17, RP4_K3_17, RP4_11S2xS2.

Freedman's classification [Freedman 82] of simply connected closed topological 4-manifolds settled the 4-dimensional topological Poincaré conjecture. The 4-dimensional smooth Poincaré conjecture, however, is still wide open: does the 4-dimensional sphere S^4 have a unique differentiable structure, or are there exotic 4-spheres that are homeomorphic but not diffeomorphic to S^4? The categories PL and DIFF coincide in dimension 4 (see the survey [Milnor 11] and the references therein), and the 4-dimensional smooth Poincaré conjecture therefore can be rephrased on the level of triangulations: is every triangulation of S^4 PL homeomorphic to the boundary of the 5-simplex?

Exotic structures on simply connected 4-manifolds have been intensively studied over the past years. One main task has been to find smaller and smaller k and l such that the connected sum $(\#k\,\mathbb{C}\mathbf{P}^2)\#(-\#l\,\mathbb{C}\mathbf{P}^2)$ has exotic structures. While it is now known [Akhmedov and Park 10] that $\mathbb{C}\mathbf{P}^2\#(-\#2\,\mathbb{C}\mathbf{P}^2)$ admits (infinitely many) exotic structures, the remaining interesting open cases are $\mathbb{C}\mathbf{P}^2\#(-\mathbb{C}\mathbf{P})$, $\mathbb{C}\mathbf{P}^2$, and S^4 (the smooth Poincaré conjecture), as well as $\mathrm{S}^2 \times \mathrm{S}^2$.

The example CP2 in Table 7 is the unique vertex-minimal nine-vertex triangulation of $\mathbb{C}\mathbf{P}^2$ from [Kühnel and Banchoff 83], and it carries the standard PL structure.

The constructions of exotic structures are often delicate, and it is not straightforward to derive corresponding triangulations. A very explicit example, though not simply connected, can be found in [Kreck 84].

Theorem 5.9. [Kreck 84] *The* 4*-dimensional manifolds* $\mathbb{R}\mathbf{P}^4\#K3$ *and* $\mathbb{R}\mathbf{P}^4\#(S^2 \times S^2)^{\#11}$ *are homeomorphic but not*

diffeomorphic, the constitutive components being equipped with the standard smooth structures.

A 17-vertex triangulation K3_17 of the K3 surface with the standard PL type is from [Spreer and Kühnel 11]. A vertex-minimal 16-vertex triangulation K3_16 of the topological K3 surface was previously found in [Casella and Kühnel 01]. It is not clear whether the two triangulations are PL homeomorphic—we tried bistellar flips to establish a PL homeomorphism between these two triangulations, but without success.

A vertex-minimal 16-vertex triangulation RP4 of $\mathbb{R}\,\mathbf{P}^4$ was obtained in [Lutz 05] by applying bistellar flips to the 31-vertex standard triangulation of $\mathbb{R}\,\mathbf{P}^4$ from [Kühnel 87].

Let K and L be two triangulated 4-manifolds with n and m vertices, respectively. Their connected sum $K\#L$ (or $K\#-L$ in cases in which orientation of the components matters) is obtained from K and L by removing a 4-simplex from each of the triangulations and then gluing together the remainders along the respective boundaries. The resulting triangulation $K\#L$ then has $n+m-5$ vertices. Triangulations of connected sums $(S^2\times S^2)^{\#k}$, $k\geq 2$, are therefore easily constructed from a vertex-minimal 11-vertex triangulation of $S^2\times S^2$ [Lutz 05] by taking connected sums and then applying bistellar flips to reduce the numbers of vertices. In this way, we obtained triangulations of $(S^2\times S^2)^{\#2}$ with 12 vertices (vertex-minimal; cf. [Lutz 05]), of $(S^2\times S^2)^{\#3}$ with 14 vertices, of $(S^2\times S^2)^{\#5}$ with 16 vertices, of $(S^2\times S^2)^{\#6}$ with 16 vertices, of $(S^2\times S^2)^{\#9}$ with 18 vertices, and of $(S^2\times S^2)^{\#11}$ with 20 vertices.

Theorem 5.10. *Let $\mathbb{R}\,\mathbf{P}^4$, $K3$, and $(S^2\times S^2)^{\#11}$ be equipped with their standard PL structures. The PL 4-manifold $\mathbb{R}\,\mathbf{P}^4\#K3$ has a triangulation* RP4_K3_17 *with $16+17-5=28$ vertices, and the PL 4-manifold $\mathbb{R}\,\mathbf{P}^4\#(S^2\times S^2)^{\#11}$ has a triangulation* RP4_11S2xS2 *with $16+20-5=31$ vertices. While the underlying topological manifolds of these PL manifolds are homeomorphic, the respective triangulations are not PL homeomorphic.*

By Theorem 5.10, we see that homeomorphic but not PL homeomorphic triangulations of 4-manifolds can be constructed with only a few vertices. (Most likely, the explicit numbers of vertices in Theorem 5.10 can be further reduced with bistellar flips. However, this would require a rather extensive search, which is beyond the scope of this article.)

Theorem 5.11. *The examples* CP2, RP4, K3_16, K3_17, RP4_K3_17, *and* RP4_11S2xS2 *have perfect discrete Morse functions with* 3, 5, 24, 24, 27, *and* 27 *critical cells, respectively.*

Interestingly, the computed discrete Morse spectra of K3_16 and K3_17 look rather similar. The same can be said for the pair RP4_K3_17 and RP4_11S2xS2.

5.8. Hom Complexes

Examples: Hom_C5_K4, Hom_n9_655_compl_K4, Hom_C6_compl_K5_small, Hom_C6_compl_K5, Hom_C5_K5.

Hom complexes of certain graphs provide interesting examples of prodsimplicial manifolds [Csorba and Lutz 06]. The prodsimplicial structure allows us to triangulate these manifolds easily without adding new vertices.

The 3-dimensional Hom complex Hom_C5_K4 is a triangulation of the 3-dimensional real projective space $\mathbb{R}\,\mathbf{P}^3$; the Hom complex Hom_n9_655_compl_K4 triangulates $(S^2\times S^1)^{\#13}$.

The 4-dimensional example Hom_C6_compl_K5_small with $f=(33,379,1786,2300,920)$ is obtained from Hom_C6_compl_K5 with

$$f=(1920,30780,104520,126000,50400)$$

via bistellar flips. Both examples triangulate $(S^2\times S^2)^{\#29}$, the first with computed normalized average 63.92, the latter with normalized average 83.0. In only three out of 2000 runs did we find the discrete Morse vector (1, 1, 59, 0, 1) for Hom_C6_compl_K5, and never the optimum (1, 0, 58, 0, 1). In contrast, both the lex and the rev_lex heuristics yielded (1, 0, 58, 0, 1). In order to keep the list short, Table 8 lists only 10 random runs for Hom_C6_compl_K5.

The Hom complex Hom_C5_K5 with $f=(1020,25770,143900,307950,283200,94400)$ is a triangulation of $S^3\times S^2$ with normalized average 4.6.

5.9. Higher-Dimensional Manifolds

Examples: poincare, hyperbolic_dodecahedral_space, SU2_SO3, non_PL, RP5_24, S2xpoincare, _HP2.

The 16-vertex triangulation poincare [Björner and Lutz 00, Björner and Lutz 03] of the Poincaré homology 3-sphere with f-vector $f=(16,106,180,90)$ has the binary icosahedral group as its fundamental group. Since this group is acyclic, we have $c_2\geq 2$, and therefore every discrete Morse vector for poincare must have at least six critical cells, with (1, 2, 2, 1) being the optimal discrete Morse vector according to Table 4; cf. also [Lewiner et al. 03b].

For hyperbolic_dodecahedral_space [Lutz et al. 09], the 21-vertex triangulation of the Weber–Seifert hyperbolic dodecahedral space [Weber and Seifert 33] with face vector $f=(21,193,344,172)$, the best discrete Morse vector we found is (1, 4, 4, 1). The fundamental group of this manifold can be presented with four generators; see Table 12. To the best of our knowledge, it is an open problem whether the

Heegaard genus of the hyperbolic dodecahedral space is 3 or 4. Equivalently (cf. Theorem 4.7), we do not know whether there exists some triangulation with Morse vector (1, 3, 3, 1).

The product triangulation `S2xpoincare` of S^2 (taken as the boundary of a tetrahedron) with `poincare` again has the binary icosahedral group as its fundamental group, inherited from `poincare`; for constructing product triangulations, see [Lutz 03] and references therein. The best discrete Morse vector we found for this examples in 103 out of 1000 runs is (1, 2, 3, 3, 2, 1). (Table 9 list only 20 random runs for `S2xpoincare` to keep the list short.)

The two 5-manifolds SU(2)/ SO(3) and $\mathbb{R}\,\mathbf{P}^5$ have homology vectors $(\mathbb{Z}, 0, \mathbb{Z}, \mathbb{Z}, 0, \mathbb{Z})$ and $(\mathbb{Z}, \mathbb{Z}_2, 0, \mathbb{Z}_2, 0, \mathbb{Z})$ and triangulations `SU2_SO3` with 13 vertices and `RP5_24` with 24 vertices, respectively [Lutz 99, Lutz 05]. The 15-vertex triangulation `_HP2` of an 8-dimensional manifold "like a quaternionic projective plane" from [Brehm and Kühnel 92] has homology $(\mathbb{Z}, 0, 0, 0, \mathbb{Z}, 0, 0, 0, \mathbb{Z})$.

Theorem 5.12. *The triangulations* `SU2_SO3`*,* `RP5_24`*, and* `_HP2` *have optimal discrete Morse vectors* (1, 0, 1, 1, 0, 1)*,* (1, 1, 1, 1, 1, 1)*, and* (1, 0, 0, 0, 1, 0, 0, 0, 1)*, respectively.*

The 18-vertex non-PL triangulation `non_PL` [Björner and Lutz 00] of the 5-dimensional sphere S^5 admits (1, 0, 0, 2, 2, 1) as discrete Morse vector.

5.10. Random 2-Complexes and Fundamental Groups

`Example: rand2_n25_p0.328`

In generalization of the classical Erdős–Rényi model for random graphs [Erdős and Rényi 60], [Linial and Meshulam 06] considered random 2-dimensional complexes with complete 1-skeleton on n vertices; every triangle with vertices from the set $\{1, \ldots, n\}$ is then added with probability p independently. Let $Y(n, p)$ be the set of such complexes. For the elements of $Y(n, p)$, Linial and Meshulam proved a sharp threshold for the vanishing of the first homology with $\mathbb{Z}_2$-coefficients,

$$\lim_{n\to\infty} \text{Prob}[\, Y \in Y(n,p) \mid H_1(Y, \mathbb{Z}_2) = 0\,] = \begin{cases} 1 & \text{for } p = \dfrac{2\log n + \omega(n)}{n}, \\ 0 & \text{for } p = \dfrac{2\log n - \omega(n)}{n}, \end{cases}$$

for every function $\omega(n) \to \infty$ as $n \to \infty$ (as long as $p \in [0, 1]$). Replacing homological connectivity by simple connectivity, it was shown in [Babson et al. 10] that there is a range for p for which asymptotically almost surely, the complexes $Y \in Y(n, p)$ have nontrivial fundamental groups with trivial abelianizations,

$$\lim_{n\to\infty} \text{Prob}[\, Y \in Y(n,p) \mid \pi_1(Y) = 0\,] = 1$$

for

$$p \geq \left(\frac{3\log n + \omega(n)}{n}\right)^{1/2},$$

with the exponent $1/2$ being best possible.

More recently, it was shown in [Cohen et al. 12] that for $p \ll n^{-1}$ asymptotically almost surely, the complexes $Y \in Y(n, p)$ admit a discrete Morse function with no critical 2-cells. See also the recent results in higher dimensions in [Aronshtam et al. 13], where the authors consider the case $p = c \cdot n^{-1}$.

The example `rand2_n25_p0.328` on $n = 25$ vertices from Table 3 with homology $(\mathbb{Z}, 0, \mathbb{Z}^{475})$ has 751 triangles, each chosen with probability $p = 0.328$. We found the optimal discrete Morse vector (1, 0, 475) in 275 out of 10 000 runs.

According to [Seifert and Threlfall 34, Section 44], a presentation of the fundamental group of a simplicial complex can be obtained via the edge-path group. For this, a spanning tree of edges is deleted from the 1-skeleton of the complex, and each remaining edge contributes a generator to the fundamental group, while each triangle of the 2-skeleton contributes a relator.[4]

We used the GAP command `SimplifiedFpGroup` to simplify the edge-path group presentation of the fundamental group. The heuristic `SimplifiedFpGroup` does not necessarily output a minimal presentation of a finitely presented group with the minimal number of generators and relators. Nevertheless, even in the case of huge complexes, `SimplifiedFpGroup` succeeded in recognizing trivial, cyclic (one generator, at most one relator), or free groups (no relators). In Table 12, we list for the examples of Tables 3–10 the number of generators and the number of relators of the initial presentation, the number of generators and the number of relators of the simplified group, along with the resulting fundamental group and the time it took for the simplification. In Tables 12–14, $F(k)$ denotes the free group with k generators.

In Tables 13 and 14, we list resulting fundamental groups for random 2-complexes with 25 and 50 vertices, respectively. In these tables, the Linial–Meshulam threshold can be observed quite nicely. For $p = \frac{2\log 25}{25} \approx 0.26$ and $p = \frac{2\log 50}{50} \approx 0.16$, 73 and 75 out of 100 random examples with respectively $n = 25$ and $n = 50$ vertices had trivial fundamental groups. Thus, for these values of p, we are in precisely the range of the slope of the threshold. While most of the examples in Tables 13 and 14

[4] An implementation is available at http://page.math.tu-berlin.de/~lutz/stellar/FundamentalGroup.

have free fundamental groups, we found "nonfree" examples (for which their presentations could not be simplified to remove all relators) in the range in which p is slightly smaller than $3/n$, the value for which [Linial et al. 10] constructed acyclic examples as sum complexes.

In our experiments, we did not observe the Babson–Hoffmann–Kahle examples with nontrivial fundamental groups that have trivial abelianizations. However, as pointed out by Kenyon, "exceptional events" can occur for random groups when n is small, while the asymptotic behavior can be rather different; cf. [Ollivier 05, pp. 42–43].

5.11. Vertex-Homogeneous Complexes and the Evasiveness Conjecture

`Example: contractible_vertex_homogeneous.`

As remarked in [Kahn et al. 84], we have the following implications for simplicial complexes:

$$\text{nonevasive} \Rightarrow \text{collapsible} \Rightarrow \text{contractible} \Rightarrow \mathbb{Z}\text{-acyclic}.$$

The evasiveness conjecture [Kahn et al. 84] for simplicial complexes states that every vertex-homogeneous nonevasive simplicial complex is a simplex. The first examples of vertex-homogeneous $\mathbb{Z}$-acyclic simplicial complexes different from simplices were given by Oliver (cf. [Kahn et al. 84]); see [Lutz 02] for further examples. While join products and other constructions can be used to derive vertex-homogeneous contractible simplicial complexes different from simplices, nontrivial vertex-homogeneous nonevasive examples cannot be obtained in this way [Welker 99].

The smallest example of a contractible vertex-homogeneous simplicial complex from [Lutz 02], `contractible_vertex_homogeneous`, is 11-dimensional with

$$f = (60, 1290, 12380, 58935, 148092, 220840, 211740, 136155, 59160, 16866, 2880, 225).$$

The best discrete Morse vector we found with the `lex` and the `rev_lex` heuristics for this contractible space is $(1, 0, 0, 4, 8, 4, 0, 0, 0, 0, 0, 0)$. We do not know whether the example is collapsible.

6. APPENDIX A: COMPLEXES ON WHICH OUR HEURISTIC FAILS

In this section, we construct simplicial complexes on which our random approach will most likely fail to guess the right Morse vector. In these examples, exponentially many rounds (in the number of facets) of the program may be necessary before an optimal Morse vector shows up as output. Such pathological examples can be produced in any positive dimension. The crucial idea is highlighted by the following 1-dimensional case.

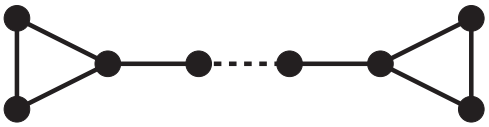

FIGURE 4. The graph A_{k+6} with $k - 1 + 6$ vertices.

Example 6.1. Let k be a positive integer. Let A_{k+6} be the graph consisting of two cycles of length 3 that are connected by a path of k edges; see Figure 4. Since A_{k+6} has no free edge, our algorithm picks an edge e uniformly at random and removes it. The final outcome depends on this choice, and on this choice only:

1. If e belongs to the k-edge path, it is easy to see that the program will always output the discrete Morse vector $(2, 3)$.
2. If instead e belongs to one of the two (empty) triangles, then the program will always output the Morse vector $(1, 2)$.

Hence, the algorithm finds a perfect Morse function on A_{k+6} with probability $p = \frac{6}{6+k}$. For large k, the algorithm will most likely (i.e., with probability $q = \frac{k}{6+k}$) return a Morse vector that is "off by 2," displaying five critical cells instead of three.

Example 6.2. Let s be a positive integer. Let $B_{k+6}(s)$ be a bouquet of s copies of A_{k+6}. An optimal discrete Morse function on $B_{k+6}(s)$ has Morse vector $(1, 2s)$. Finding a discrete Morse function on $B_{k+6}(s)$ is the same as (independently) finding s discrete Morse functions on the s copies of A_{k+6}. Therefore, the probability of getting the optimal Morse vector on $B_{k+6}(s)$ is p^s, where $p = \frac{6}{6+k}$. This corresponds to putting together s optimal Morse functions on the different copies of A_{k+6}, or in other words, to picking one favorable edge in each copy of A_{k+6}. For $0 \le i \le s$, the probability that the program outputs the Morse vector $(1 + i, 2s + i)$ is $\binom{s}{i} p^{s-i}(1 - p)^i$, corresponding to i "bad" choices and $s - i$ "good" choices.

To show that an analogous phenomenon occurs also in higher dimensions, let us recall a classical definition in PL topology.

Definition 6.3. Let C be a d-dimensional complex. A *stacking operation* on C is the transition from C to $C' = (C - \text{star}(\sigma, C)) \cup \hat{\sigma} * \text{link}(\sigma, C)$, where σ is an arbitrary facet of C and $\hat{\sigma}$ is a new vertex (e.g., the barycenter of σ). More generally, we say that C' *is obtained from* C *by stacking* if some finite sequence of stacking operations leads from C to C'.

Each stacking operation adds d facets; so a complex obtained by performing s stacking operations on a d-simplex has exactly $ds + 1$ facets.

Lemma 6.4. *If C' is obtained from a simplex by stacking, then C' is shellable. In particular, it is endocollapsible: for every facet σ of C', there is a sequence of elementary collapses that reduces $C' - \sigma$ to $\partial C'$.*

In dimension $d \geq 3$, there is no guarantee that every sequence of elementary collapses on $C' - \sigma$ can be continued until one reaches $\partial C'$. This is why in the following example, probabilities have to be estimated rather than computed.

Example 6.5. Let d, k be positive integers, with $k \equiv 1 \bmod d$. Take a disjoint union of $d + 1$ edges $e_0, \ldots, e_d$ and a d-simplex S (with facets $F_0, \ldots, F_d$). For each i in $\{0, \ldots, d\}$, glue in the boundary of the join $F_i * e_i$. The resulting complex C^d is homotopy equivalent to a bouquet of $d + 1$ spheres of dimension d; the homotopy is just the contraction of the central simplex S to a point. Let C^d_k be a complex obtained by stacking the simplex S exactly s times, so that S gets subdivided into $k = ds + 1$ simplices of the same dimension.

Note first of all that C^1_k coincides with the A_{k+6} of Example 6.1. For an example $C^2_{2\cdot 5+1}$, see Figure 5.

Since C^d_k has no free $(d-1)$-faces, our algorithm starts by removing some d-face σ at random. We have two possible cases:

1. With probability $\frac{k}{(d+2)(d+1)+k}$, we pick σ from the subdivision of the central simplex.

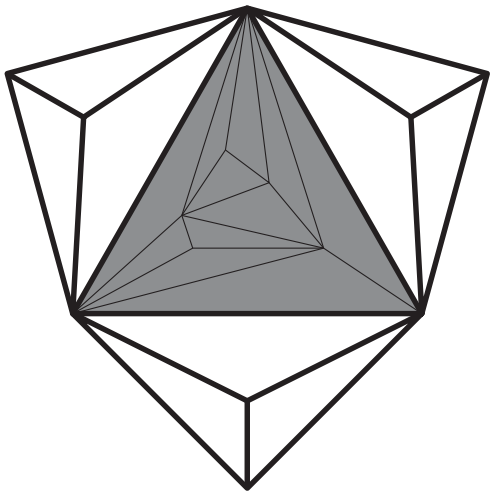

FIGURE 5. An example $C^2_{2\cdot 5+1}$ with the central 2-simplex S (in gray) subdivided five times and the boundary edges of S blocked by three empty tetrahedra.

2. With probability $\frac{(d+2)(d+1)}{(d+2)(d+1)+k}$, we pick σ from one of the d-spheres.

In the first case, some sequence of elementary collapses reduces $C^d_k - \sigma$ onto $C^d - S$. So our algorithm will output a Morse vector that is either $(1, 0, \ldots, 0, 1, d + 2)$ or a (componentwise) larger vector, but certainly not the vector $(1, 0, \ldots, 0, 0, d + 1)$.

Thus the probability of obtaining the optimal Morse vector $(1, 0, \ldots, 0, 0, d + 1)$ is positive, but less than or equal to $\frac{(d+2)(d+1)}{(d+2)(d+1)+k}$. As k gets larger, this upper bound gets smaller and smaller.

Example 6.6. By taking a bouquet of w copies of Example 6.5, we obtain a complex $B^d_k(w)$. For $d = 1$, $B^d_k(w)$ coincides with the $B_{k+6}(w)$ of Example 6.2. The probability of seeing the perfect Morse vector $(1, 0, \ldots, 0, 0, (d + 1)w)$ on $B^d_k(w)$ is less than or equal to $\left(\frac{(d+2)(d+1)}{(d+2)(d+1)+k}\right)^w$.

For practical purposes, it is useful to understand how this probability grows with respect to the number N of facets. In fact, given a complex with N facets, we would like to know concretely how often we should run the algorithm before we can expect an optimal Morse vector to appear among the outputs.

For the sake of brevity, we do the calculations in dimension one—but similar estimates can be easily derived in all dimensions. The graph constructed in Example 6.2 has $N = (6 + k)w$ edges. To study the probability $(\frac{6}{6+k})^w$ of finding an optimal Morse function, we should regard N as a constant, write w as $\frac{N}{6+k}$, and study the function

$$P(k) = \left(\frac{6}{6+k}\right)^{\frac{N}{6+k}}.$$

Classical calculus reveals that the function $x \mapsto x^x = e^{x \log x}$ is strictly decreasing on the interval $(0, e^{-1})$ and strictly increasing on (e^{-1}, ∞). It achieves its minimum at e^{-1}. So given any bijection $g : (0, \infty) \to (0, 1)$, the function $y \mapsto g(y)^{g(y)}$ achieves its minimum at the (unique) point y such that $g(y) = e^{-1}$. Applying this to $g(y) = \frac{6}{6+y}$, we get

$$\min_{y\in\mathbb{R}} \left(\frac{6}{6+y}\right)^{\frac{N}{6+y}} = \min_{y\in\mathbb{R}} \left(g(y)^{g(y)\frac{N}{6}}\right) = \left(\min_{y\in\mathbb{R}} g(y)^{g(y)}\right)^{\frac{N}{6}}$$
$$= \left((e^{-1})^{e^{-1}}\right)^{\frac{N}{6}} = e^{-\frac{N}{6e}}.$$

Yet we wanted to minimize the function $P(k)$ over the integers, not over the reals. However, if we choose the integer k such that $\frac{6}{6+k}$ is close to e^{-1}, we can see that the value of $P(k)$ is close to $P(e^{-1})$. The minimum is in fact achieved at $k = 10$.

Thus $P(k)$ can be as small as e^{-cN}, where c is some constant "close" to $\frac{1}{6e}$. It is in fact $c = \frac{1}{16}(\log 8 - \log 3) \approx 0.0613018$.

7. APPENDIX B: LIBRARY AND TABLES

Tables 3–10 list computational results for the examples of Section 5.

For each example, we present the discrete Morse spectrum we experimentally observed in a certain number of runs (usually 10 000, when not otherwise stated; sometimes, we did fewer runs for reasons concerning either excessive computation time or excessive variance of the spectrum).

Let $c_{\approx}$ and $c_{\approx}^N$ be the average numbers of critical cells for the vectors in the approximated discrete Morse spectrum and the approximated normalized discrete Morse spectrum, respectively. The longer we run RANDOM DISCRETE MORSE, the better the approximation of c_σ by $c_{\approx}$ and of c_σ^N by $c_{\approx}^N$ will become—and possibly optimal discrete Morse vectors will show up.

In Tables 3–10, optimal discrete Morse vectors are highlighted in bold. We wrote an output vector in italics if it is the best we could find with our algorithm and we do not know whether it is optimal.

For Table 11, we replaced the random choices in our algorithm with a deterministic lexicographic or reverse lexicographic choice. The labeling of the vertices of course now plays a role; see [Adiprasito et al. 14] for a discussion of a randomized version (by randomly renumbering vertices first) of `lex` and `rev_lex`.

All computations were run on a cluster of 2.6 GHz processors.

Name of Example/Homology/ f-Vector/$c^N_{\approx}$	Distribution of Obtained Discrete Morse Vectors in 10000 Rounds		Time for Hasse Diagram/ Time per Round (in Hour:Min:Sec.Frac)
`dunce_hat`	**(1,1,1)**:	10000	0.004
($\mathbb{Z}$, 0, 0)			0.00024
(8, 24, 17)			
3.0000			
`d2n12g6`	**(1,12,1)**:	9722	0.004
($\mathbb{Z}$, $\mathbb{Z}^{12}$, $\mathbb{Z}$)	(2, 13, 1):	277	0.00076
(12, 66, 44)	(3, 14, 1):	1	
14.0000			
`regular_2_21_23_1`	**(1,30,1)**:	9337	0.008
($\mathbb{Z}$, $\mathbb{Z}^{30}$, $\mathbb{Z}$)	(2, 31, 1):	649	0.00201
(21, 147, 98)	(3, 32, 1):	14	
32.0000			
`rand2_n25_p0.328`	(1, 3, 478):	2185	0.228
($\mathbb{Z}$, 0, $\mathbb{Z}^{475}$)	(1, 4, 479):	1874	0.00428
(25, 300, 751)	(1, 2, 477):	1847	
482.9032	(1, 5, 480):	1265	
	(1, 1, 476):	1048	
	(1, 6, 481):	704	
	(1, 7, 482):	318	
	(1,0,475):	275	
	(1, 8, 483):	140	
	(2, 4, 478):	66	
	(2, 5, 479):	66	
	(2, 6, 480):	54	
	(2, 7, 481):	41	
	(1, 9, 484):	40	
	(2, 3, 477):	24	
	(2, 8, 482):	21	
	(1, 10, 485):	12	
	(2, 9, 483):	8	
	(1, 11, 486):	4	
	(2, 10, 484):	3	
	(2, 11, 485):	3	
	(3, 6, 479):	1	
	(3, 8, 481):	1	
`dunce_hat_in_3_ball`	**(1,0,0,0)**:	10000	0.004
($\mathbb{Z}$, 0, 0, 0)			0.00049
(8, 25, 30, 12)			
1.0000			
`Barnette_sphere` (nonpolytopal)	**(1,0,0,1)**:	10000	0.004
($\mathbb{Z}$, 0, 0, $\mathbb{Z}$)			0.00060
(8, 27, 38, 19)			
2.0000			
`B_3_9_18` (nonshellable ball)	**(1,0,0,0)**:	10000	0.004
($\mathbb{Z}$, 0, 0, 0)			0.00073
(9, 33, 43, 18)			
1.0000			
`trefoil_arc`	**(1,0,0,0)**:	9529	0.004
($\mathbb{Z}$, 0, 0, 0)	(1, 1, 1, 0):	466	0.00158
(12, 58, 85, 38)	(1, 2, 2, 0):	5	
1.0952			

TABLE 3. Library of triangulations and discrete Morse spectra (part 1).

Name of Example/Homology/ f-Vector/$c^N_{\approx}$	Distribution of Obtained Discrete Morse Vectors in 10000 Rounds		Time for Hasse Diagram/ Time per Round (in Hour:Min:Sec.Frac)
`trefoil`	**(1,0,0,1)**:	9617	0.004
$(\mathbb{Z}, 0, 0, \mathbb{Z})$	(1, 1, 1, 1):	377	0.00208
(13, 69, 112, 56)	(1, 2, 2, 1):	6	
2.0778			
`rudin` (Rudin's ball)	**(1,0,0,0)**:	10000	0.004
$(\mathbb{Z}, 0, 0, 0)$			0.00107
(14, 66, 94, 41)			
1.0000			
`double_trefoil_arc`	**(1,1,1,0)**:	7080	0.012
$(\mathbb{Z}, 0, 0, 0)$	(1, 2, 2, 0):	2698	0.00329
(15, 93, 145, 66)	(1, 3, 3, 0):	197	
3.6260	(2, 3, 2, 0):	18	
	(1, 4, 4, 0):	6	
	(2, 4, 3, 0):	1	
`poincare`	**(1,2,2,1)**:	9073	0.016
$(\mathbb{Z}, 0, 0, \mathbb{Z})$	(1, 3, 3, 1):	864	0.00400
(16, 106, 180, 90)	(1, 4, 4, 1):	45	
6.1952	(2, 4, 3, 1):	7	
	(2, 3, 2, 1):	6	
	(1, 5, 5, 1):	5	
`double_trefoil`	(1, 1, 1, 1):	4550	0.012
$(\mathbb{Z}, 0, 0, \mathbb{Z})$	**(1,0,0,1)**:	3972	0.00408
(16, 108, 184, 92)	(1, 2, 2, 1):	1316	
3.5338	(1, 3, 3, 1):	145	
	(1, 4, 4, 1):	8	
	(2, 3, 2, 1):	7	
	(2, 4, 3, 1):	2	
`triple_trefoil_arc`	**(1,2,2,0)**:	6027	0.024
$(\mathbb{Z}, 0, 0, 0)$	(1, 3, 3, 0):	3220	0.00528
(17, 127, 208, 97)	(1, 4, 4, 0):	569	
5.9352	(1, 5, 5, 0):	77	
	(2, 4, 3, 0):	51	
	(2, 3, 2, 0):	42	
	(2, 5, 4, 0):	10	
	(1, 6, 6, 0):	4	
`triple_trefoil`	(1, 2, 2, 1):	4427	0.024
$(\mathbb{Z}, 0, 0, \mathbb{Z})$	**(1,1,1,1)**:	3080	0.00640
(18, 143, 250, 125)	(1, 3, 3, 1):	1911	
5.9898	(1, 4, 4, 1):	430	
	(1, 5, 5, 1):	57	
	(2, 3, 2, 1):	40	
	(2, 4, 3, 1):	33	
	(2, 5, 4, 1):	15	
	(2, 6, 5, 1):	4	
	(1, 6, 6, 1):	3	

TABLE 4. Library of triangulations and discrete Morse spectra (continued).

Name of Example/Homology/ f-Vector/$c^N_{\approx}$	Distribution of Obtained Discrete Morse Vectors in 10000 Rounds		Time for Hasse Diagram/ Time per Round (in Hour:Min:Sec.Frac)
`hyperbolic_dodecahedral_space`	*(1,4,4,1)*:	4792	0.036
$(\mathbb{Z}, \mathbb{Z}_5^3, 0, \mathbb{Z})$	(1, 5, 5, 1):	3338	0.01017
(21, 190, 338, 169)	(1, 6, 6, 1):	1245	
11.4672	(1, 7, 7, 1):	326	
	(2, 5, 4, 1):	82	
	(2, 6, 5, 1):	80	
	(1, 8, 8, 1):	62	
	(2, 7, 6, 1):	45	
	(2, 8, 7, 1):	18	
	(1, 9, 9, 1):	8	
	(2, 9, 8, 1):	3	
	(1, 10, 10, 1):	1	
`S_3_50_1033` (random)	**(1,0,0,1)**:	7087	0.900
$(\mathbb{Z}, 0, 0, \mathbb{Z})$	(1, 1, 1, 1):	1383	0.153
(50, 1083, 2066, 1033)	(1, 2, 2, 1):	697	
3.1966	(1, 3, 3, 1):	386	
	(1, 4, 4, 1):	189	
	(1, 5, 5, 1):	118	
	(1, 6, 6, 1):	42	
	(2, 4, 3, 1):	25	
	(2, 3, 2, 1):	18	
	(2, 5, 4, 1):	14	
	(1, 7, 7, 1):	12	
	(2, 6, 5, 1):	9	
	(1, 8, 8, 1):	9	
	(2, 7, 6, 1):	4	
	(2, 8, 7, 1):	3	
	(1, 10, 10, 1):	2	
	(2, 9, 8, 1):	1	
	(1, 9, 9, 1):	1	
`S_3_100_4850` (cyclic polytope)	**(1,0,0,1)**:	10000	17.829
$(\mathbb{Z}, 0, 0, \mathbb{Z})$			1.883
(100, 4950, 9700, 4850)			
2.0000			
`600_cell`	**(1,0,0,1)**:	10000	0.364
$(\mathbb{Z}, 0, 0, \mathbb{Z})$			0.076
(120, 720, 1200, 600)			
2.0000			
`non_4_2_colorable`	(4, 15, 12, 1):	2	1.728
$(\mathbb{Z}, 0, 0, \mathbb{Z})$	(1, 7, 7, 1):	1	0.254
(167, 1579, 2824, 1412)	(2, 12, 11, 1)	1	[10 rounds]
25.2	(2, 13, 12, 1)	1	
	(3, 13, 11, 1)	1	
	(4, 16, 13, 1):	1	
	(5, 14, 10, 1):	1	
	(5, 18, 14, 1):	1	
	(7, 20, 14, 1):	1	
`Hom_C5_K4` ($\mathbb{R}\,\mathbf{P}^3$)	**(1,1,1,1)**:	9753	1.864
$(\mathbb{Z}, \mathbb{Z}_2, 0, \mathbb{Z})$	(1, 2, 2, 1):	240	0.379
(240, 1680, 2880, 1440)	(2, 3, 2, 1):	6	
4.0496	(1, 3, 3, 1):	1	

TABLE 5. Library of triangulations and discrete Morse spectra (continued).

Name of Example/Homology/ f-Vector/$c^N_{\approx}$	Distribution of Obtained Discrete Morse Vectors in 10000 Rounds		Time for Hasse Diagram/ Time per Round (in Hour:Min:Sec.Frac)
`trefoil_bsd`	**(1,0,0,1)**:	9902	1.716
$(\mathbb{Z}, 0, 0, \mathbb{Z})$	(1, 1, 1, 1):	95	0.308
(250, 1594, 2688, 1344)	(1, 2, 2, 1):	3	
2.0202			
`knot`	*(1,1,1,0)*:	9414	1.576
$(\mathbb{Z}, 0, 0, 0)$	(1, 2, 2, 0):	560	0.813
(380, 1929, 2722, 1172)	(2, 3, 2, 0):	15	
3.1194	(1, 3, 3, 0):	9	
	(2, 4, 3, 0):	2	
`nc_sphere`	(1, 1, 1, 1):	7902	3.228
$(\mathbb{Z}, 0, 0, \mathbb{Z})$	(1, 2, 2, 1):	1809	0.470
(381, 2309, 3856, 1928)	(1, 3, 3, 1):	234	
4.4760	(1, 4, 4, 1):	25	
	(1,0,0,1):	12	
	(2, 3, 2, 1):	9	
	(1, 6, 6, 1):	3	
	(2, 4, 3, 1):	3	
	(2, 5, 4, 1):	2	
	(1, 5, 5, 1):	1	
`double_trefoil_bsd`	(1, 1, 1, 1):	4819	4.376
$(\mathbb{Z}, 0, 0, \mathbb{Z})$	**(1,0,0,1)**:	4274	0.811
(400, 2608, 4416, 2208)	(1, 2, 2, 1):	833	
3.3414	(1, 3, 3, 1):	64	
	(1, 4, 4, 1):	4	
	(2, 3, 2, 1):	4	
	(2, 4, 3, 1):	2	
`bing`	(1, 1, 1, 0):	9764	2.788
$(\mathbb{Z}, 0, 0, 0)$	(1, 2, 2, 0):	217	1.398
(480, 2511, 3586, 1554)	**(1,0,0,0)**:	7	
3.0456	(1, 3, 3, 0):	6	
	(2, 3, 2, 0):	6	
`triple_trefoil_bsd`	(1, 2, 2, 1):	4793	8.024
$(\mathbb{Z}, 0, 0, \mathbb{Z})$	*(1,1,1,1)*:	3390	1.456
(536, 3536, 6000, 3000)	(1, 3, 3, 1):	1543	
5.7352	(1, 4, 4, 1):	208	
	(1, 5, 5, 1):	22	
	(2, 3, 2, 1):	20	
	(2, 4, 3, 1):	17	
	(1, 6, 6, 1):	3	
	(2, 5, 4, 1):	3	
	(1, 8, 8, 1):	1	
`S_3_1000_2990` (stacked sphere)	**(1,0,0,1)**:	10000	8.444
$(\mathbb{Z}, 0, 0, \mathbb{Z})$			1.498
(1000, 3990, 5980, 2990)			
2.0000			
`Hom_n9_655_compl_K4` $((S^2 \times S^1)^{\#13})$	**(1,13,13,1)**:	67	5:39.809
$(\mathbb{Z}, \mathbb{Z}^{13}, \mathbb{Z}^{13}, \mathbb{Z})$	(1, 14, 14, 1):	20	45.682
(3096, 22104, 38016, 19008)	(1, 15, 15, 1):	5	[100 rounds]
28.68	(2, 14, 13, 1):	5	
	(2, 15, 14, 1):	2	
	(2, 16, 15, 1):	1	

TABLE 6. Library of triangulations and discrete Morse spectra (continued).

Name of Example/Homology/ f-Vector/$c^N_{\approx}$	Distribution of Obtained Discrete Morse Vectors in 10000 Rounds		Time for Hasse Diagram/ Time per Round (in Hour:Min:Sec.Frac)
`CP2`	**(1,0,1,0,1)**:	9994	0.012
$(\mathbb{Z}, 0, \mathbb{Z}, 0, \mathbb{Z})$	(1, 1, 2, 0, 1):	6	0.00226
(9, 36, 84, 90, 36)			
3.0012			
`RP4`	**(1,1,1,1,1)**:	9765	0.056
$(\mathbb{Z}, \mathbb{Z}_2, 0, \mathbb{Z}_2, 0)$	(1, 2, 2, 1, 1):	136	0.01678
(16, 120, 330, 375, 150)	(1, 1, 2, 2, 1):	89	
5.0490	(1, 3, 3, 1, 1):	5	
	(1, 2, 3, 2, 1):	3	
	(1, 1, 3, 3, 1):	1	
	(2, 3, 2, 1, 1):	1	
`K3_16` (unknown PL type)	**(1,0,22,0,1)**:	6702	0.168
$(\mathbb{Z}, 0, \mathbb{Z}^{22}, 0, \mathbb{Z})$	(1, 1, 23, 0, 1):	2615	0.04417
(16, 120, 560, 720, 288)	(1, 2, 24, 0, 1):	506	
24.8218	(1, 3, 25, 0, 1):	60	
	(1, 0, 23, 1, 1):	31	
	(1, 1, 24, 1, 1):	15	
	(1, 0, 24, 2, 1):	13	
	(1, 0, 25, 3, 1):	9	
	(1, 2, 25, 1, 1):	6	
	(2, 3, 24, 0, 1):	5	
	(1, 0, 26, 4, 1):	4	
	(1, 1, 26, 3, 1):	4	
	(1, 4, 26, 0, 1):	4	
	(1, 0, 27, 5, 1):	3	
	(1, 1, 27, 4, 1):	3	
	(1, 2, 27, 3, 1):	2	
	(1, 3, 26, 1, 1):	2	
	(1, 1, 28, 5, 1):	2	
	(1, 2, 28, 4, 1):	1	
	(1, 3, 27, 2, 1):	1	
	(1, 2, 29, 5, 1):	1	
	(1, 2, 26, 2, 1):	1	
`K3_17` (standard PL type)	**(1,0,22,0,1)**:	6337	0.196
$(\mathbb{Z}, 0, \mathbb{Z}^{22}, 0, \mathbb{Z})$	(1, 1, 23, 0, 1):	2939	0.05093
(17, 135, 610, 780, 312)	(1, 2, 24, 0, 1):	618	
24.8978	(1, 3, 25, 0, 1):	78	
	(1, 4, 26, 0, 1):	8	
	(1, 0, 23, 1, 1):	6	
	(1, 0, 25, 3, 1):	4	
	(2, 3, 24, 0, 1):	3	
	(1, 0, 24, 2, 1):	2	
	(1, 0, 26, 4, 1):	2	
	(1, 1, 24, 1, 1):	1	
	(1, 2, 27, 3, 1):	1	
	(1, 5, 27, 0, 1):	1	

TABLE 7. Library of triangulations and discrete Morse spectra (continued).

Name of Example/Homology/ f-Vector/$c^N_{\approx}$	Distribution of Obtained Discrete Morse Vectors in 10000 Rounds		Time for Hasse Diagram/ Time per Round (in Hour:Min:Sec.Frac)
`RP4_K3_17`	**(1,1,23,1,1)**:	55	0.392
$(\mathbb{Z}, \mathbb{Z}_2, \mathbb{Z}^{22}, \mathbb{Z}_2, 0)$	(1, 2, 24, 1, 1):	24	0.0754
(28, 245, 930, 1150, 460)	(1, 3, 25, 1, 1):	8	[100 rounds]
28.56	(1, 1, 24, 2, 1):	3	
	(1, 2, 25, 2, 1):	2	
	(1, 4, 26, 1, 1):	2	
	(1, 1, 26, 4, 1):	1	
	(1, 3, 26, 2, 1):	1	
	(1, 3, 27, 3, 1):	1	
	(1, 3, 28, 4, 1):	1	
	(1, 5, 30, 4, 1):	1	
	(2, 4, 25, 1, 1):	1	
`RP4_11S2xS2`	**(1,1,23,1,1)**:	51	0.496
$(\mathbb{Z}, \mathbb{Z}_2, \mathbb{Z}^{22}, \mathbb{Z}_2, 0)$	(1, 2, 24, 1, 1):	29	0.0945
(31, 283, 1052, 1295, 518)	(1, 3, 25, 1, 1):	14	[100 rounds]
28.46	(1, 1, 24, 2, 1):	1	
	(1, 1, 25, 3, 1):	1	
	(1, 1, 26, 4, 1):	1	
	(1, 2, 27, 4, 1):	1	
	(1, 4, 26, 1, 1):	1	
	(2, 4, 25, 1, 1):	1	
`Hom_C6_compl_K5_small` $((S^2 \times S^2)^{\#29})$	(1, 1, 59, 0, 1):	33	1.460
$(\mathbb{Z}, 0, \mathbb{Z}^{58}, 0, \mathbb{Z})$	(1, 2, 60, 0, 1):	30	0.348
(33, 379, 1786, 2300, 920)	(1, 3, 61, 0, 1):	12	[100 rounds]
63.92	**(1,0,58,0,1)**:	11	
	(1, 4, 62, 0, 1):	5	
	(1, 5, 63, 0, 1):	3	
	(1, 6, 64, 0, 1):	3	
	(2, 3, 60, 0, 1):	1	
	(1, 4, 63, 1, 1):	1	
	(1, 7, 65, 0, 1):	1	
`Hom_C6_compl_K5` $((S^2 \times S^2)^{\#29})$	(1, 10, 68, 0, 1):	3	2:18:33.603
$(\mathbb{Z}, 0, \mathbb{Z}^{58}, 0, \mathbb{Z})$	(1, 17, 75, 0, 1):	2	19:26.475
(1920, 30780, 104520, 126000, 50400)	(1, 7, 65, 0, 1):	1	[10 rounds]
83.0	(1, 8, 66, 0, 1):	1	([2000 rounds], Sec. 5.8)
	(1, 9, 67, 0, 1):	1	
	(1, 11, 69, 0, 1):	1	
	(2, 16, 73, 0, 1):	1	
`SU2_SO3`	**(1,0,1,1,0,1)**:	9369	0.124
$(\mathbb{Z}, 0, \mathbb{Z}, \mathbb{Z}, 0, \mathbb{Z})$	(1, 0, 2, 2, 0, 1):	554	0.03250
(13, 78, 286, 533, 468, 156)	(1, 1, 2, 1, 0, 1):	35	
4.1354	(1, 0, 3, 3, 0, 1):	32	
	(1, 1, 3, 2, 0, 1):	5	
	(1, 0, 4, 4, 0, 1):	4	
	(1, 2, 3, 1, 0, 1):	1	

TABLE 8. Library of triangulations and discrete Morse spectra (continued).

Name of Example/Homology/ f-Vector/$c^N_{\approx}$	Distribution of Obtained Discrete Morse Vectors in 10000 Rounds		Time for Hasse Diagram/ Time per Round (in Hour:Min:Sec.Frac)
non_PL	*(1,0,0,2,2,1)*:	9383	0.324
$(\mathbb{Z}, 0, 0, 0, 0, \mathbb{Z})$	(1, 0, 0, 3, 3, 1):	441	0.06964
(18, 139, 503, 904, 783, 261)	(1, 0, 1, 3, 2, 1):	134	
6.1328	(1, 0, 0, 4, 4, 1):	23	
	(1, 0, 1, 4, 3, 1):	12	
	(1, 0, 2, 4, 2, 1):	2	
	(1, 0, 0, 5, 5, 1):	2	
	(1, 0, 2, 5, 3, 1):	1	
	(1, 1, 2, 3, 2, 1):	1	
	(1, 0, 4, 6, 2, 1):	1	
RP5_24	**(1,1,1,1,1,1)**:	9181	1.800
$(\mathbb{Z}, \mathbb{Z}_2, 0, \mathbb{Z}_2, 0, \mathbb{Z})$	(1, 1, 2, 2, 1, 1):	344	0.429
(24, 273, 1174, 2277, 2028, 676)	(1, 2, 2, 1, 1, 1):	315	
6.1766	(1, 1, 1, 2, 2, 1):	97	
	(1, 2, 3, 2, 1, 1):	21	
	(1, 1, 3, 3, 1, 1):	15	
	(1, 3, 3, 1, 1, 1):	9	
	(1, 1, 2, 3, 2, 1):	6	
	(1, 2, 2, 2, 2, 1):	5	
	(1, 1, 1, 3, 3, 1):	3	
	(1, 3, 3, 2, 2, 1):	1	
	(1, 3, 4, 2, 1, 1):	1	
	(2, 3, 2, 1, 1, 1):	1	
	(2, 4, 3, 1, 1, 1):	1	
S2xpoincare	(1, 3, 4, 3, 2, 1):	6	46.611
$(\mathbb{Z}, 0, \mathbb{Z}, \mathbb{Z}, 0, \mathbb{Z})$	(1, 4, 6, 4, 2, 1):	3	8.460
(64, 1156, 5784, 11892, 10800, 3600)	*(1,2,3,3,2,1)*:	2	[20 rounds]
15.70	(1, 2, 4, 4, 2, 1):	2	([1000 rounds], Sec. 5.9)
	(1, 3, 5, 4, 2, 1):	2	
	(1, 3, 6, 5, 2, 1):	2	
	(1, 2, 5, 5, 2, 1):	1	
	(1, 4, 7, 5, 2, 1):	1	
	(1, 3, 7, 6, 2, 1):	1	
S_5_100_472 (stacked sphere)	**(1,0,0,0,0,1)**:	10000	1.188
$(\mathbb{Z}, 0, 0, 0, 0, \mathbb{Z})$			0.309
(100, 579, 1430, 1895, 1416, 472)			
2.0000			
Hom_C5_K5 ($S^3 \times S^2$)	**(1,0,1,1,0,1)**:	7	16:16:14.156
$(\mathbb{Z}, 0, \mathbb{Z}, \mathbb{Z}, 0, \mathbb{Z})$	(1, 0, 2, 2, 0, 1):	2	2:53:37.911
(1020, 25770, 143900, 307950, 283200, 94400)	(1, 1, 2, 1, 0, 1):	1	[10 rounds]
4.6			

TABLE 9. Library of triangulations and discrete Morse spectra (continued).

Name of Example/Homology/ f-Vector/$c^N_{\approx}$	Distribution of Obtained Discrete Morse Vectors in 10000 Rounds		Time for Hasse Diagram/ Time per Round (in Hour:Min:Sec.Frac)
_HP2	**(1,0,0,0,1,0,0,0,1)**:	9474	11.348
($\mathbb{Z}$, 0, 0, 0, $\mathbb{Z}$, 0, 0, 0, $\mathbb{Z}$)	(1, 0, 0, 1, 2, 0, 0, 0, 1):	459	1.425
(15, 105, 455, 1365, 3003, 4515, 4230,	(1, 0, 0, 2, 3, 0, 0, 0, 1):	46	
2205, 490)	(1, 0, 0, 3, 4, 0, 0, 0, 1):	7	
3.1212	(1, 0, 0, 0, 2, 1, 0, 0, 1):	4	
	(1, 0, 1, 2, 2, 0, 0, 0, 1):	3	
	(1, 0, 1, 4, 4, 0, 0, 0, 1):	2	
	(1, 0, 1, 1, 1, 0, 0, 0, 1):	1	
	(1, 0, 0, 1, 5, 3, 0, 0, 1):	1	
	(1, 0, 2, 2, 1, 0, 0, 0, 1):	1	
	(1, 0, 0, 1, 6, 4, 0, 0, 1):	1	
	(1, 0, 0, 4, 5, 0, 0, 0, 1):	1	
contractible_vertex_homogeneous	(1, 3, 38, 98, 83, 20, 0, . . . , 0):	1	11:42:37.994
($\mathbb{Z}$, 0, 0, 0, 0, 0, 0, 0, 0, 0, 0, 0)	(1, 3, 42, 72, 43, 10, 0, . . . , 0):	1	1:39:02.745
(60, 1290, 12380, 58935, 148092,	(1, 4, 34, 80, 64, 14, 0, . . . , 0):	1	[10 rounds]
220840, 211740, 136155, 59160,	(1, 4, 53, 87, 56, 18, 0, . . . , 0):	1	
16866, 2880, 225)	(1, 5, 63, 110, 61, 9, 0, . . . , 0):	1	
273.6	(1, 5, 70, 139, 92, 18, 0, . . . , 0):	1	
	(1, 6, 42, 115, 108, 29, 0, . . . , 0):	1	
	(1, 8, 75, 160, 113, 20, 0, . . . , 0):	1	
	(1, 9, 66, 124, 89, 22, 0, . . . , 0):	1	
	(1, 13, 74, 144, 97, 14, 0, . . . , 0):	1	

TABLE 10. Library of triangulations and discrete Morse spectra (continued).

Name of Example	lex	rev_lex
dunce_hat	**(1,1,1)**	**(1,1,1)**
d2n12g6	**(1,12,1)**	**(1,12,1)**
regular_2_21_23_1	**(1,30,1)**	**(1,30,1)**
rand2_n25_p0.328	**(1,0,475)**	**(1,0,475)**
dunce_hat_in_3_ball	**(1,0,0,0)**	**(1,0,0,0)**
Barnette_sphere	**(1,0,0,1)**	**(1,0,0,1)**
B_3_9_18 (nonshellable ball)	**(1,0,0,0)**	**(1,0,0,0)**
trefoil_arc	(1, 2, 2, 0)	**(1,0,0,0)**
trefoil	(1, 2, 2, 1)	**(1,0,0,1)**
rudin (Rudin's ball)	**(1,0,0,0)**	**(1,0,0,0)**
double_trefoil_arc	(1, 3, 3, 0)	(1, 2, 2, 0)
poincare	**(1,2,2,1)**	**(1,2,2,1)**
double_trefoil	(1, 3, 3, 1)	(1, 1, 1, 1)
triple_trefoil_arc	(1, 4, 4, 0)	(1, 3, 3, 0)
triple_trefoil	(1, 4, 4, 1)	(1, 2, 2, 1)
hyperbolic_dodecahedral_space	*(1,4,4,1)*	(1, 5, 5, 1)
S_3_50_1033 (random)	**(1,0,0,1)**	**(1,0,0,1)**
S_3_100_4850 (cyclic polytope)	**(1,0,0,1)**	**(1,0,0,1)**
600_cell	**(1,0,0,1)**	**(1,0,0,1)**
non_4_2_colorable	(1, 30, 30, 1)	**(1,0,0,1)**
Hom_C5_K4 ($\mathbb{R}\,\mathbf{P}^3$)	**(1,1,1,1)**	**(1,1,1,1)**
trefoil_bsd	(1, 2, 2, 1)	**(1,0,0,1)**
knot	*(1,1,1,0)*	*(1,1,1,0)*
nc_sphere	(1, 2, 2, 1)	(1, 1, 1, 1)
double_trefoil_bsd	(1, 3, 3, 1)	(1, 1, 1, 1)
bing	(1, 1, 1, 0)	(1, 1, 1, 0)
triple_trefoil_bsd	(1, 4, 4, 1)	(1, 3, 3, 1)
S_3_1000_2990 (stacked sphere)	**(1,0,0,1)**	**(1,0,0,1)**
Hom_n9_655_compl_K4 ($((S^2 \times S^1)^{\#13}$)	(2,14,13,1)	**(1,13,13,1)**
CP2	**(1,0,1,0,1)**	**(1,0,1,0,1)**
RP4	**(1,1,1,1,1)**	**(1,1,1,1,1)**
K3_16 (unknown PL type)	**(1,0,22,0,1)**	**(1,0,22,0,1)**
K3_17 (standard PL type)	**(1,0,22,0,1)**	**(1,0,22,0,1)**
RP4_K3_17	**(1,1,23,1,1)**	**(1,1,23,1,1)**
RP4_11S2xS2	**(1,1,23,1,1)**	**(1,1,23,1,1)**
Hom_C6_compl_K5_small ($((S^2 \times S^2)^{\#29}$)	**(1,0,58,0,1)**	**(1,0,58,0,1)**
Hom_C6_compl_K5 ($((S^2 \times S^2)^{\#29}$)	**(1,0,58,0,1)**	**(1,0,58,0,1)**
SU2_SO3	**(1,0,1,1,0,1)**	**(1,0,1,1,0,1)**
non_PL	*(1,0,0,2,2,1)*	*(1,0,0,2,2,1)*
RP5_24	**(1,1,1,1,1,1)**	**(1,1,1,1,1,1)**
S2xpoincare	*(1,2,3,3,2,1)*	*(1,2,3,3,2,1)*
S_5_100_472 (stacked sphere)	**(1,0,0,0,0,1)**	**(1,0,0,0,0,1)**
Hom_C5_K5 ($S^3 \times S^2$)	**(1,0,1,1,0,1)**	**(1,0,1,1,0,1)**
_HP2	**(1,0,0,0,1,0,0,0,1)**	**(1,0,0,0,1,0,0,0,1)**
contractible_vertex_homogeneous	*(1,0,0,4,8,4,0,0,0,0,0,0)*	*(1,0,0,4,8,4,0,0,0,0,0,0)*

TABLE 11. Discrete Morse vectors with lex and rev_lex heuristics.

Name of Example	Ge.	Re.	SGe.	SRe.	F. Gr.	Time
dunce_hat	17	17	0	0	0	0.036
d2n12g6	55	44	12	1	12 gen.	0.132
regular_2_21_23_1	127	98	30	1	30 gen.	0.304
rand2_n25_p0.328	276	751	0	0	0	0.876
dunce_hat_in_3_ball	18	30	0	0	0	0.044
Barnette_sphere	20	38	0	0	0	0.048
B_3_9_18 (nonshellable ball)	25	43	0	0	0	0.048
trefoil_arc	47	85	0	0	0	0.092
trefoil	57	112	0	0	0	0.084
rudin (Rudin's ball)	53	94	0	0	0	0.060
double_trefoil_arc	79	145	0	0	0	0.148
poincare	91	180	2	2	2 gen.	0.104
double_trefoil	93	184	0	0	0	0.160
triple_trefoil_arc	111	208	0	0	0	0.164
triple_trefoil	126	250	0	0	0	0.156
hyperbolic_dodecahedral_space	170	338	4	5	4 gen.	0.276
S_3_50_1033 (random)	1034	2066	0	0	0	6.372
S_3_100_4850 (cyclic polytope)	4851	9700	0	0	0	2:38.918
600_cell	601	1200	0	0	0	2.220
non_4_2_colorable	1413	2824	0	0	0	12.644
Hom_C5_K4 ($\mathbb{R}\,\mathbf{P}^3$)	1441	2880	1	1	$\mathbb{Z}_2$	13.492
trefoil_bsd	1345	2688	0	0	0	11.292
knot	1550	2722	0	0	0	12.536
nc_sphere	1929	3856	0	0	0	23.509
double_trefoil_bsd	2209	4416	0	0	0	30.002
bing	2032	3586	0	0	0	22.877
triple_trefoil_bsd	3001	6000	0	0	0	57.947
S_3_1000_2990 (stacked sphere)	2991	5980	0	0	0	58.099
Hom_n9_655_compl_K4 ($(S^2 \times S^1)^{\#13}$)	19009	38016	13	0	F(13)	59:14.006
CP2	28	84	0	0	0	0.036
RP4	105	330	1	1	$\mathbb{Z}_2$	0.200
K3_16 (unknown PL type)	105	560	0	0	0	0.344
K3_17 (standard PL type)	119	610	0	0	0	0.372
RP4_K3_17	218	930	1	1	$\mathbb{Z}_2$	0.408
RP4_11S2xS2	253	1052	1	1	$\mathbb{Z}_2$	0.472
Hom_C6_compl_K5_small ($(S^2 \times S^2)^{\#29}$)	347	1786	0	0	0	2.420
Hom_C6_compl_K5 ($(S^2 \times S^2)^{\#29}$)	28861	104520	0	0	0	3:57:09.873
SU2_SO3	66	286	0	0	0	0.180
non_PL	122	503	0	0	0	0.368
RP5_24	250	1174	1	1	$\mathbb{Z}_2$	1.244
S2xpoincare	1093	5784	2	2	2 gen.	22.493
S_5_100_472 (stacked sphere)	480	1430	0	0	0	2.380
Hom_C5_K5 ($S^3 \times S^2$)	24751	143900	0	0	0	5:22:22.520
_HP2	91	455	0	0	0	0.356
contractible_vertex_homogeneous	1231	12380	0	0	0	46.431

TABLE 12. Simplified presentations of fundamental groups with GAP. Here Ge. is the number of generators, Re. the number of relators of the initial presentation, SGe. the number of generators, SRe. the number of relators of the simplified group, F. Gr. the resulting fundamental group, and Time the time it took for the simplification.

p	0	$F(1)$	$F(2)$	$F(3)$	$F(4)$	$F(5)$	$F(6)$	$F(7)$	$F(8)$	$F(9)$	$F(10)$	$F(\geq 11)$	"nonfree"
0.40	100	0	0	0	0	0	0	0	0	0	0	0	0
0.39	100	0	0	0	0	0	0	0	0	0	0	0	0
0.38	99	1	0	0	0	0	0	0	0	0	0	0	0
0.37	100	0	0	0	0	0	0	0	0	0	0	0	0
0.36	98	2	0	0	0	0	0	0	0	0	0	0	0
0.35	96	3	1	0	0	0	0	0	0	0	0	0	0
0.34	99	1	0	0	0	0	0	0	0	0	0	0	0
0.33	97	3	0	0	0	0	0	0	0	0	0	0	0
0.32	95	5	0	0	0	0	0	0	0	0	0	0	0
0.31	97	3	0	0	0	0	0	0	0	0	0	0	0
0.30	97	3	0	0	0	0	0	0	0	0	0	0	0
0.29	88	10	1	1	0	0	0	0	0	0	0	0	0
0.28	83	16	1	0	0	0	0	0	0	0	0	0	0
0.27	83	15	2	0	0	0	0	0	0	0	0	0	0
0.26	73	19	8	0	0	0	0	0	0	0	0	0	0
0.25	73	21	3	2	1	0	0	0	0	0	0	0	0
0.24	66	27	6	1	0	0	0	0	0	0	0	0	0
0.23	39	39	20	1	1	0	0	0	0	0	0	0	0
0.22	31	39	20	8	2	0	0	0	0	0	0	0	0
0.21	23	24	35	7	7	2	1	0	1	0	0	0	0
0.20	16	33	26	16	5	3	1	0	0	0	0	0	0
0.19	8	18	24	16	18	7	7	1	0	1	0	0	0
0.18	9	13	24	18	19	8	3	1	4	1	0	0	0
0.17	2	6	10	20	9	21	13	10	5	3	0	1	0
0.16	0	1	3	13	12	17	21	9	6	4	6	8	0
0.15	0	0	0	4	16	5	10	14	10	10	7	24	0
0.14	0	0	0	0	0	1	3	5	11	13	5	62	0
0.13	0	0	0	0	0	0	1	1	0	3	6	89	0
0.12	0	0	0	0	0	0	0	0	0	0	3	96	1
0.11	0	0	0	0	0	0	0	0	0	0	0	92	8
0.10	0	0	0	0	0	0	0	0	0	0	0	98	2
0.09	0	0	0	0	0	0	0	0	0	0	0	99	1
0.08	0	0	0	0	0	0	0	0	0	0	0	100	0
0.07	0	0	0	0	0	0	0	0	0	0	0	100	0
0.06	0	0	0	0	0	0	0	0	0	0	0	100	0

TABLE 13. Distribution of fundamental groups for random 2-complexes with 25 vertices (100 runs for each p).

p	0	$F(1)$	$F(2)$	$F(3)$	$F(4)$	$F(5)$	$F(6)$	$F(7)$	$F(8)$	$F(9)$	$F(10)$	$F(\geq 11)$	"nonfree"
0.25	100	0	0	0	0	0	0	0	0	0	0	0	0
0.24	100	0	0	0	0	0	0	0	0	0	0	0	0
0.23	99	1	0	0	0	0	0	0	0	0	0	0	0
0.22	99	1	0	0	0	0	0	0	0	0	0	0	0
0.21	97	3	0	0	0	0	0	0	0	0	0	0	0
0.20	98	2	0	0	0	0	0	0	0	0	0	0	0
0.19	96	4	0	0	0	0	0	0	0	0	0	0	0
0.18	90	10	0	0	0	0	0	0	0	0	0	0	0
0.17	81	18	1	0	0	0	0	0	0	0	0	0	0
0.16	75	24	1	0	0	0	0	0	0	0	0	0	0
0.15	68	26	4	2	0	0	0	0	0	0	0	0	0
0.14	43	27	21	8	1	0	0	0	0	0	0	0	0
0.13	16	39	31	10	2	1	1	0	0	0	0	0	0
0.12	8	15	22	19	25	6	3	1	1	0	0	0	0
0.11	1	4	9	10	16	20	21	8	7	1	1	2	0
0.10	0	0	1	4	5	6	13	17	11	15	10	18	0
0.09	0	0	0	0	1	0	2	0	4	4	5	84	0
0.08	0	0	0	0	0	0	0	0	0	0	0	100	0
0.07	0	0	0	0	0	0	0	0	0	0	0	100	0
0.06	0	0	0	0	0	0	0	0	0	0	0	95	5
0.05	0	0	0	0	0	0	0	0	0	0	0	86	14
0.04	0	0	0	0	0	0	0	0	0	0	0	100	0
0.03	0	0	0	0	0	0	0	0	0	0	0	100	0
0.02	0	0	0	0	0	0	0	0	0	0	0	100	0
0.01	0	0	0	0	0	0	0	0	0	0	0	100	0

TABLE 14. Distribution of fundamental groups for random 2-complexes with 50 vertices (100 runs for each p).

ACKNOWLEDGMENTS

Thanks to Karim Adiprasito, Herbert Edelsbrunner, Alex Engström, Michael Joswig, Roy Meshulam, Konstantin Mischaikow, Vidit Nanda, and John M. Sullivan for helpful discussions and remarks.

FUNDING

Bruno Benedetti's research was supported by the Swedish Research Council, grant "Triangulerade Mångfalder, Knutteori i diskrete Morseteori," and the DFG Collaborative Research Center TRR 109, "Discretization in Geometry and Dynamics″." Frank H. Lutz's research was supported by the DFG Research Group "Polyhedral Surfaces," by VILLUM FONDEN through the Experimental Mathematics Network, and by the Danish National Research Foundation (DNRF) through the Centre for Symmetry and Deformation.

REFERENCES

[Adiprasito et al. 14] K. Adiprasito, B. Benedetti, and F. H. Lutz. "Random Discrete Morse Theory II and a Collapsible 5-Manifold Different from the 5-Ball." In preparation, 2014.

[Akbulut and Kirby 85] S. Akbulut and R. Kirby. "A Potential Smooth Counterexample In Dimension 4 to the Poincaré Conjecture, the Schoenflies Conjecture, and the Andrews–Curtis Conjecture." *Topology* 24 (1985), 375–390.

[Akhmedov and Park 10] A. Akhmedov and B. D. Park. "Exotic Smooth Structures on Small 4-Manifolds with Odd Signatures." *Invent. Math.* 181, (2010), 577–603.

[Altshuler et al. 96] A. Altshuler, J. Bokowski, and P. Schuchert. "Neighborly 2-Manifolds with 12 Vertices." *J. Comb. Theory, Ser. A* 75 (1996), 148–162.

[Aronshtam et al. 13] L. Aronshtam, N. Linial, T. Łuczak, and R. Meshulam. "Collapsibility and Vanishing of Top Homology in Random Simplicial Complexes." *Discrete Comput. Geom.* 49 (2013), 317–334 .

[Babson et al. 10] E. Babson, C. Hoffman, and M. Kahle. "The Fundamental Group of Random 2-Complexes." *J. Am. Math. Soc.* 24 (2010), 1–28.

[Bagchi and Datta 05] B. Bagchi and B. Datta. "Combinatorial Triangulations of Homology Spheres." *Discrete Math.* 305, 1–17 (2005).

[Barnette 73] D. Barnette. "The Triangulations of the 3-Sphere with up to 8 Vertices." *J. Comb. Theory, Ser. A* 14 (1973), 37–52.

[Benedetti 12] B. Benedetti. "Discrete Morse Theory for Manifolds with Boundary." *Trans. Am. Math. Soc.* 364 (2012), 6631–6670.

[Benedetti 13] B. Benedetti. "Smoothing Discrete Morse Theory." arXiv:1212.0885v2, 2013.

[Benedetti and Lutz 13a] B. Benedetti and F. H. Lutz. "Knots in Collapsible and Non-Collapsible Balls." *Electron. J. Comb.* 20 No. 3, Research Paper P31, 2013.

[Benedetti and Lutz 13b] B. Benedetti and F. H. Lutz. "The Dunce Hat and a Minimal Non-extendably Collapsible 3-Ball." *Electronic Geometry Model* No. 2013.10.001. Available online (http://www.eg-models.de/2013.10.001), 2013.

[Bing 64] R. H. Bing. "Some Aspects of the Topology of 3-Manifolds Related to the Poincaré Conjecture." In *Lectures on Modern Mathematics II*, edited by T. L. Saaty, pp. 93–128. Wiley, New York, 1964.

[Björner and Lutz 00] A. Björner and F. H. Lutz. "Simplicial Manifolds, Bistellar Flips and a 16-Vertex Triangulation of the Poincaré Homology 3-Sphere." *Exp. Math.* 9 (2000), 275–289.

[Björner and Lutz 03] A. Björner and F. H. Lutz. "A 16-Vertex Triangulation of the Poincaré Homology 3-Sphere and Non-PL Spheres with Few Vertices." *Electronic Geometry Model* No. 2003.04.001. Available online (http://www.eg-models.de/2003.04.001), 2003.

[Boileau and Zieschang 84] M. Boileau and H. Zieschang. "Heegaard Genus of Closed Orientable Seifert 3-Manifolds." *Invent. Math.* 76 (1984), 455–468.

[Brehm and Kühnel 92] U. Brehm and W. Kühnel. "15-Vertex Triangulations of an 8-Manifold." *Math. Ann.* 294 (1992), 167–193.

[Casella and Kühnel 01] M. Casella and W. Kühnel. "A Triangulated K3 Surface with the Minimum Number of Vertices." *Topology* 40 (2001), 753–772.

[Chari 00] M. K. Chari. "On Discrete Morse Functions and Combinatorial Decompositions." *Discrete Math.* 217 (2000), 101–113.

[Cohen et al. 12] D. Cohen, A. Costa, M. Farber, and T. Kappeler. "Topology of Random 2-Complexes." *Discrete Comput. Geom.* 47 (2012), 117–149.

[Crowley et al. 03] K. Crowley, A. Ebin, H. Kahn, P. Reyfman, J. White, and M. Xue. "Collapsing a Simplex to a Noncollapsible Simplicial Complex." Preprint, 2003.

[Csorba and Lutz 06] P. Csorba and F. H. Lutz. "Graph Coloring Manifolds." In *Algebraic and Geometric Combinatorics, Euroconf. Math., Algebraic and Geometric Combinatorics, Anogia, Crete, Greece, 2005*, edited by C. A. Athanasiadis, V. V. Batyrev, D. I. Dais, M. Henk, and F. Santos, Contemporary Mathematics 423, pp. 51–69. American Mathematical Society, 2006.

[Dunfield and Thurston 06] N. M. Dunfield and W. P. Thurston. "Finite Covers of Random 3-Manifolds." *Invent. Math.* 166 (2006), 457–521.

[Engström 09] A. Engström. "Discrete Morse Functions from Fourier Transforms." *Exp. Math.* 18 (2009), 45–53.

[Erdős and Rényi 60] P. Erdős and A. Rényi. "On the Evolution of Random Graphs." *Publ. Math. Inst. Hung. Acad. Sci., Ser. A* 5 (1960) 17–61.

[Forman 98] R. Forman. "Morse Theory for Cell Complexes." *Adv. Math.* 134 (1998), 90–145.

[Forman 02] R. Forman. "A User's Guide to Discrete Morse Theory." *Sémin. Lothar. Comb.* 48 (2002), B48c (electronic).

[Freedman 82] M. H. Freedman. "The Topology of Four-Dimensional Manifolds." *J. Differ. Geom.* 17 (1982), 357–453.

[Goodrick 68] R. E. Goodrick. "Non-simplicially Collapsible Triangulations of I^n." *Proc. Camb. Phil. Soc.* 64 (1968), 31–36.

[Hachimori 01] M. Hachimori. "Simplicial Complex Library." Available online (http://infoshako.sk.tsukuba.ac.jp/~hachi/math/library/index_eng.html), 2001.

[Hersh 05] P. Hersh. "On Optimizing Discrete Morse Functions." *Adv. Appl. Math.* 35 (2005), 294–322.

[Joswig 04] M. Joswig. "Computing Invariants of Simplicial Manifolds." arXiv:math.AT/0401176, 2004.

[Joswig and Pfetsch 06] M. Joswig and M. E. Pfetsch. "Computing Optimal Morse Matchings." *SIAM J. Discrete Math.* 20 (2006), 11–25.

[Kahn et al. 84] J. Kahn, M. Saks, and D. Sturtevant. "A Topological Approach to Evasiveness." *Combinatorica* 4 (1984), 297–306.

[Kaibel and Pfetsch 02] V. Kaibel and M. E. Pfetsch. "Computing the Face Lattice of a Polytope from Its Vertex–Facet Incidences." *Comput. Geom.* 23 (2002), 281–290.

[Kaibel and Pfetsch 03] V. Kaibel and M. E. Pfetsch. "Some Algorithmic Problems In Polytope Theory." In *Algebra, Geometry, and Software Systems*, edited by M. Joswig and N. Takayama, pp. 23–47. Springer, 2003.

[King et al. 05] H. King, K. Knudson, and N. Mramor. "Generating Discrete Morse Functions from Point Data." *Exp. Math.* 14 (2005), 435–444.

[Kreck 84] M. Kreck. "Some Closed 4-Manifolds with Exotic Differentiable Structure." In *Algebraic Topology, Aarhus 1982*, Proc. Conference Held in Aarhus, Denmark, 1982, edited by I. Madsen and B. Oliver, Lecture Notes in Mathematics 1051, pp. 246–262. Springer, 1984.

[Kühnel 87] W. Kühnel. "Minimal Triangulations of Kummer Varieties." *Abh. Math. Sem. Univ. Hamburg* 57 (1987), 7–20.

[Kühnel and Banchoff 83] W. Kühnel and T. F. Banchoff. "The 9-Vertex Complex Projective Plane." *Math. Intell.* 5 (1983), 11–22.

[Lewiner 05] T. Lewiner. "Geometric Discrete Morse Complexes." PhD thesis, Pontifícia Universidade Católica do Rio de Janeiro, 2005.

[Lewiner et al. 03a] T. Lewiner, H. Lopes, and G. Tavares. "Optimal Discrete Morse Functions for 2-Manifolds." *Comput. Geom.* 26 (2003), 221–233.

[Lewiner et al. 03b] T. Lewiner, H. Lopes, and G. Tavares. "Toward Optimality in Discrete Morse Theory." *Exp. Math.* 12 (2003), 271–285.

[Lickorish 91] W. B. R. Lickorish. "Unshellable Triangulations of Spheres." *Eur. J. Comb.* 12 (1991), 527–530.

[Linial and Meshulam 06] N. Linial and R. Meshulam. "Homological Connectivity of Random 2-Complexes." *Combinatorica* 26 (2006), 475–487.

[Linial et al. 10] N. Linial, R. Meshulam, and M. Rosenthal. "Sum Complexes—A New Family of Hypertrees." *Discrete Comput. Geom.* 44 (2010), 622–636.

[Lutz 99] F. H. Lutz. *Triangulated Manifolds with Few Vertices and Vertex-Transitive Group Actions*. Shaker Verlag, Aachen, 1999.

[Lutz 02] F. H. Lutz. "Examples of $\mathbb{Z}$-Acyclic and Contractible Vertex-Homogeneous Simplicial Complexes." *Discrete Comput. Geom.* 27 (2002), 137–154.

[Lutz 03] F. H. Lutz. "Triangulated Manifolds with Few Vertices: Geometric 3-Manifolds." arXiv:math.GT/0311116, 2003.

[Lutz 04a] F. H. Lutz. "A Vertex-Minimal Non-shellable Simplicial 3-Ball with 9 Vertices and 18 Facets." *Electronic Geometry Model* No. 2003.05.004. Available online (http://www.eg-models.de/2003.05.004/), 2004.

[Lutz 04b] F. H. Lutz. "Small Examples of Nonconstructible Simplicial Balls and Spheres." *SIAM J. Discrete Math.* 18 (2004), 103–109.

[Lutz 05] F. H. Lutz. "Triangulated Manifolds with Few Vertices: Combinatorial Manifolds." arXiv:math.CO/0506372, 2005.

[Lutz 08] F. H. Lutz. "Combinatorial 3-Manifolds with 10 Vertices." *Beitr. Algebra Geom.* 49 (2008), 97–106.

[Lutz and Møller 14] F. H. Lutz and J. M. Møller. "A Non-(4, 2)-Colorable Triangulation of the 3-Sphere." In preparation, 2014.

[Lutz et al. 09] F. H. Lutz, T. Sulanke, and E. Swartz. "f-Vectors of 3-Manifolds." *Electron. J. Comb.* 16 (2009), research paper R13.

[Milnor 11] J. Milnor. "Differential Topology Forty-Six Years Later." *Notices Am. Math. Soc.* 58 (2011), 804–809.

[Nicolaescu 12] L. I. Nicolaescu. "Combinatorial Morse Flows Are Hard to Find." arXiv:1202.2724, 2012.

[Ollivier 05] Y. Ollivier. *A January 2005 Invitation to Random Groups*, Ensaios Matemáticos 10. Sociedade Brasileira de Matemática, Rio de Janeiro, 2005.

[Pachner 87] U. Pachner. "Konstruktionsmethoden und das kombinatorische Homöomorphieproblem für Triangulationen kompakter semilinearer Mannigfaltigkeiten." *Abh. Math. Sem. Univ. Hamburg* 57 (1987), 69–86.

[Rudin 58] M. E. Rudin. "An Unshellable Triangulation of a Tetrahedron." *Bull. Am. Math. Soc.* 64 (1958), 90–91.

[Seifert and Threlfall 34] H. Seifert and W. Threlfall. *Lehrbuch der Topologie*. B. G. Teubner, 1934.

[Spreer and Kühnel 11] J. Spreer and W. Kühnel. "Combinatorial Properties of the $K3$ Surface: Simplicial Blowups and Slicings." *Exp. Math.* 20, 201–216 (2011).

[Sulanke and Lutz 09] T. Sulanke and F. H. Lutz. "Isomorphism Free Lexicographic Enumeration of Triangulated Surfaces and 3-Manifolds." *Eur. J. Comb.* 30 (2009), 1965–1979.

[Tancer 12] M. Tancer. "Recognition of Collapsible Complexes Is NP-Complete." arXiv:1211.6254, 2012.

[Tsuruga and Lutz 13] M. Tsuruga and F. H. Lutz. "Constructing Complicated Spheres." arXiv:1302.6856, 2013.

[Weber and Seifert 33] C. Weber and H. Seifert. "Die beiden Dodekaederräume." *Math. Z.* 37 (1933), 237–253.

[Welker 99] V. Welker. "Constructions Preserving Evasiveness and Collapsibility." *Discrete Math.* 207 (1999), 243–255.

[Whitehead 39] J. H. C. Whitehead. "Simplicial Spaces, Nuclei and m-Groups." *Proc. Lond. Math. Soc., II. Ser.* 45 (1939), 243–327.

[Wotzlaw 05] R. F. Wotzlaw. "Rudin's Non-shellable Ball." *Electronic Geometry Model* No. 2004.08.001. Available online (http://www.eg-models.de/2004.08.001), 2005.